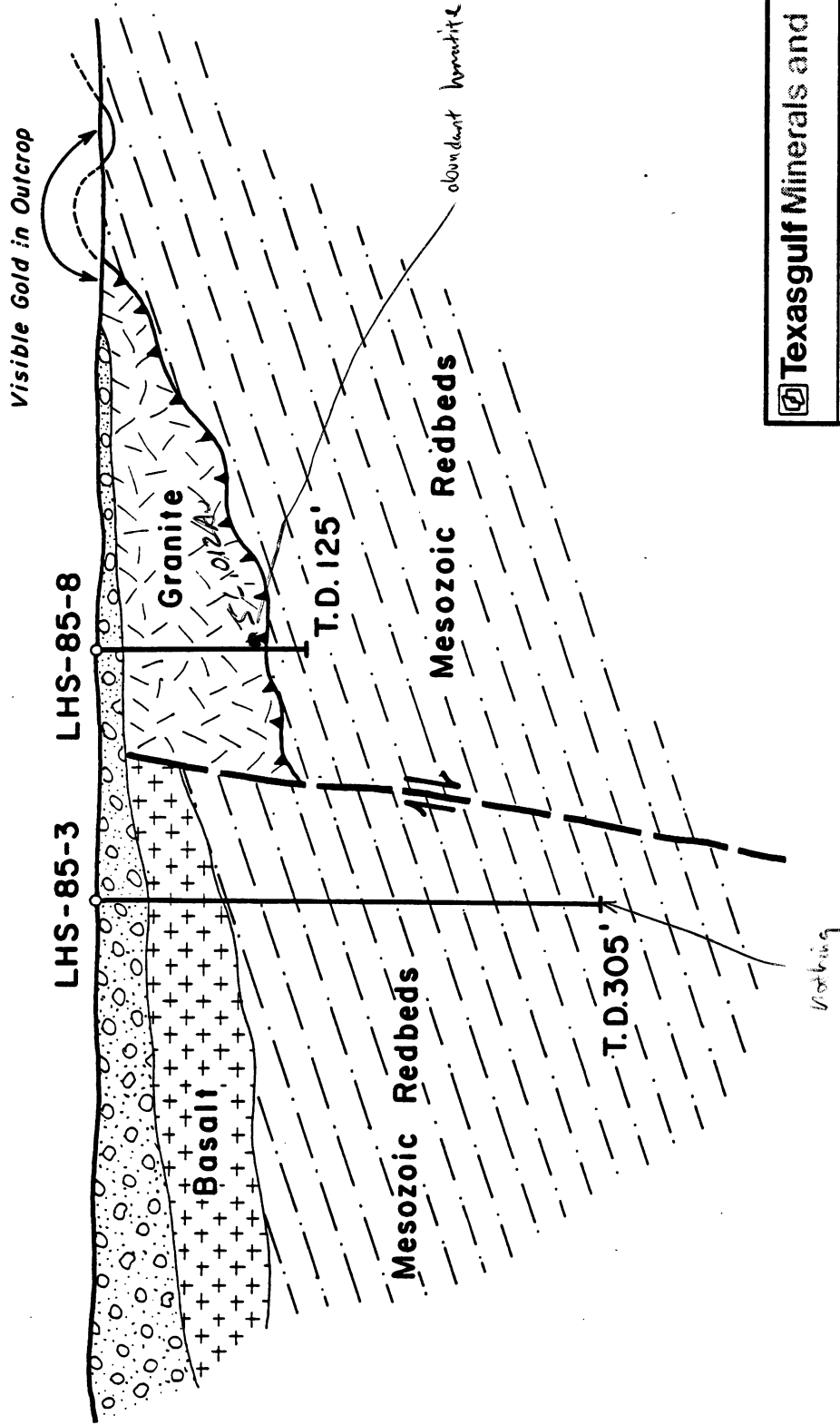


View Looking West

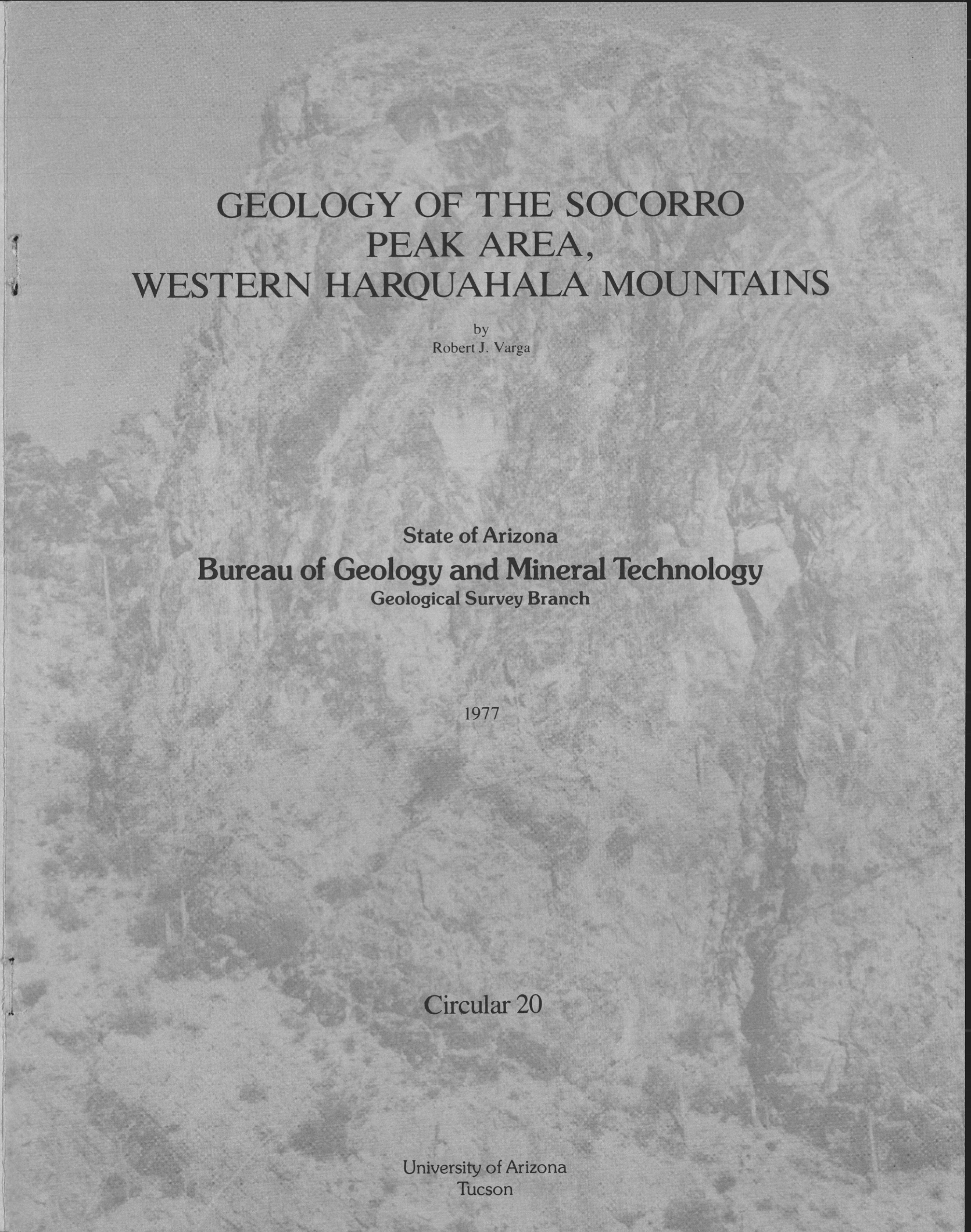


Texasgulf Minerals and Metals, Inc.

LITTLE HARQUAHALA SOUTH
CROSS SECTION
LHS-85-3 and LHS-85-8

Scale: 1 inch equals 100 feet
Date by: C. LANE
Drafted by: Asplund Oct. 15, 1985

FIG. 9



**GEOLOGY OF THE SOCORRO
PEAK AREA,
WESTERN HARQUAHALA MOUNTAINS**

by
Robert J. Varga

State of Arizona
Bureau of Geology and Mineral Technology
Geological Survey Branch

1977

Circular 20

University of Arizona
Tucson

NICOR Mineral Ventures, Inc.
Suite 12
2341 So. Friebus
Tucson, Arizona 85713

PRICE \$1.00

Material contained in this Circular may be quoted or reproduced without special permission provided appropriate acknowledgment is given to the source.

STATE OF ARIZONA
BUREAU OF GEOLOGY AND MINERAL TECHNOLOGY

William H. Drescher, Director

Geological Survey Branch

E. J. McCullough, Acting State
Geologist and Acting Assistant
Director
H. W. Peirce, Geologist
J. S. Vuich, Assistant Geologist

Mineral Technology Branch

G. H. Geiger, Acting Assistant Director
W. W. Fisher, Assistant Metallurgist
R. T. O'Haire, Associate Mineralogist
D. D. Rabb, Mining Engineer
Samuel Rudy, Assistant Metallurgist

The Arizona Bureau of Geology and Mineral Technology was established in 1977 by an act of the State legislature. This act represents a reorganization of the Arizona Bureau of Mines which first was created in 1915 and placed under the authority of the Arizona Board of Regents. This authority has not changed. The Bureau continues its service in the fields of geology, metallurgy, and mining in response to public inquiries, state agency requirements, and various research grants. In order to carry out these functions, two basic branches now are recognized:

Geological Survey Branch

This branch is charged with the responsibility of acquiring, disseminating, and applying basic geologic data that are designed to (a) enhance our understanding of Arizona's general geologic and mineralogic history and to assist in determining the short and long range influences these have on human activity, and (b) assist in developing an understanding of the controls influencing the locations of metallic, nonmetallic and mineral fuel resources in Arizona.

Mineral Technology Branch

This branch conducts research and investigations into, and provides information about, the development of Arizona's mineral resources, including the mining, metallurgical processing, and utilization of metallic and nonmetallic mineral deposits. These activities are directed toward the efficient and safe recovery of Arizona's mineral resources as well as insuring that recovery and treatment methods will be compatible with the basic environmental needs of the state.

- Miller, F. K., 1966. Structure and petrology of the southern half of the Plomosa Mountains, Yuma County, Arizona (Ph.D. thesis): Palo Alto, Stanford Univ., 173 p.
- _____, 1970. Geologic map of the Quartzsite quadrangle, Yuma County, Arizona: U. S. Geol. Survey Map GQ-841.
- _____, and McKee, E. H., 1971. Thrust and strike-slip faulting in the Plomosa Mountains, southwestern Arizona: Geol. Soc. America Bull., v. 82, p. 717-722.
- Moore, R. T., 1972. Geology of the Virgin and Beaverdam Mountains, Arizona: Arizona Bur. Mines Bull. 186, 63 p.
- Noble, L. F., 1922. A section of the Paleozoic formations of the Grand Canyon at the Bass Trail: U. S. Geol. Survey Prof. Paper 131, p. 23-73.
- Reesor, J. E., 1970. Some aspects of structural evolution and regional setting in part of the Shuswap Metamorphic Complex: Geol. Assoc. Canada Spec. Paper 6, p. 73-86.
- Shackelford, T. J., 1975. Late Tertiary gravity sliding in the Rawhide Mountains, western Arizona (abs.): Geol. Soc. America Abstracts with Programs, v. 7, p. 372-373.
- Streckeisen, A. L., Chairman, 1973. Plutonic rocks: Classification and nomenclature recommended by the IUGS Subcommittee on the Systematics of Igneous Rocks: Geotimes, v. 18, no. 10, p. 26-30.
- Varga, R. J., 1976. Stratigraphy and Superposed deformation of a Paleozoic and Mesozoic sequence in the Harquahala Mountains, Arizona (M.S. thesis): Tucson, Univ. of Arizona, 61 p.
- _____, 1977. Structural relations in the western Harquahala Mountains, west-central Arizona (abs.): Geol. Soc. America Abs. with Programs, v. 9, p. 520-521.
- Wilson, E. D., 1960. Geologic map of Yuma County, Arizona (scale 1:375,000): Tucson, Arizona Bur. Mines.
- _____, 1962. A resume of the geology of Arizona: Arizona Bur. Mines Bull. 171, 140 p.
- _____, and Moore, R. T., 1959. Structure of Basin and Range Province in Arizona: Ariz. Geol. Soc. Guidebook II, p. 89-106.

GEOLOGY OF THE SOCORRO PEAK AREA, WESTERN HARQUAHALA MOUNTAINS

by
Robert J. Varga

State of Arizona
Bureau of Geology and Mineral Technology
Geological Survey Branch

1977

Circular 20

SUMMARY

A thick sequence of Paleozoic (1,258 m) and Mesozoic (≥ 300 m) sedimentary rocks is recognized in the Socorro Peak area of the western Harquahala Mountains. These strata are lithologically similar and herein correlated to specific formations of both Colorado Plateau and southeastern Arizona nomenclature. Formations designated to represent the mapped sedimentary units include Cambrian Bolsa Quartzite (106 m), Mississippian Redwall Limestone (115 m), Permian-Pennsylvanian Supai Formation (365 m), Permian Coconino Sandstone (335 m), Permian Kaibab Limestone (335 m), and Triassic Moenkopi Formation(?) (≥ 300 m). Crystalline rocks include biotite augen gneiss and post-Triassic(?), muscovite-bearing granite.

The existence of Paleozoic rocks in western Arizona is consistent with earlier stratigraphic models which show this area as a "sag" during the Paleozoic between the Cordilleran Geosyncline to the north and the Sonoran Geosyncline to the southeast. However, the Paleozoic sequence in the Harquahala Mountains is considerably thicker than previously suggested.

Two phases of deformation are recognized within the Paleozoic and Mesozoic sequence. Gravitational tectonics in post-Triassic(?), pre-granite intrusion time is expressed in the sedimentary sequence as large-scale, steeply-inclined to recumbent folds and primarily "younger on older" faults. Direction of tectonic transport during gravity gliding is determined by kinematic analysis of folds to have been S.39°E. Sigmoidal flexuring of initial deformational trends about a vertical rotational axis occurred at a time following gravitational tectonics and granite intrusion. It is suggested that the sigmoidal flexuring was the result of a component of right-lateral, strike-slip motion on high-angle faults in post-middle Miocene(?) time.

Formation of augen gneiss is pre-granitic intrusion, although the relationship of gneiss formation to gravitational tectonics in the Paleozoic and Mesozoic sequence is indeterminate from data presented in this study. The gneiss-Paleozoic sedimentary rock interface may have acted as a zone of decollement during "cascade" folding and low-angle faulting in the sedimentary sequence.

Relationships in the western Harquahala Mountains do not support models which extend Sevier (Burchfiel and Davis, 1975) and Laramide (Burchfiel and Davis, 1975; Drewes, 1976) thrust belts through west-central Arizona into the southeastern portions of the state.

REFERENCES CITED

- Anderson, C. A., and Creasey, S. C., 1958, Geology and ore deposits of the Jerome area, Yavapai County, Arizona: U. S. Geol. Survey Prof. Paper 308, 185 p.
- Armstrong, R. L., 1972, Low-angle (denudation) faults, hinterland of the Sevier Orogenic Belt, eastern Nevada and western Utah: Geol. Soc. America Bull., v. 83, p. 1729-1754.

- _____, and Hansen, Edward, 1966, Cordilleran infrastructure in the eastern Great Basin: Am. Jour. Sci., v. 264, p. 112-127.
- Blanchard, R. C., 1913, The geology of the western Buckskin Mountains, Yuma County, Arizona (M.S. thesis): New York, Columbia Univ., 80 p.
- Bryant, D. L., 1968, Diagnostic characteristics of the Paleozoic formations of southeastern Arizona: Ariz. Geol. Soc. Guidebook III, p. 33-47.
- Burchfiel, B. C., and Davis, G. A., 1975, Nature and controls of Cordilleran orogenesis, western United States: Extension of an earlier synthesis: Am. Jour. Sci., v. 275-A, p. 363-396.
- Campbell, R. B., 1970, Structural and metamorphic transitions from infrastructure to suprastructure, Cariboo Mountains, British Columbia: Geol. Assoc. Canada Spec. Paper 6, p. 67-72.
- Ciancanelli, E. V., 1965, Structural geology of the western edge of the Granite Wash Mountains, Yuma County, Arizona (M.S. thesis): Tucson, Univ. of Arizona, 70 p.
- Coney, P. J., Overview of Mesozoic-Cenozoic Cordilleran plate tectonics: Geol. Soc. America Sp. Paper (in press).
- Darton, N. H., 1910, A reconnaissance of parts of northwestern New Mexico and northern Arizona: U. S. Geol. Survey Bull. 435, 88 p.
- Davis, G. H., 1975, Gravity-induced folding off a gneiss dome complex, Rincon Mountains, Arizona: Geol. Soc. America Bull., v. 86, p. 979-990.
- _____, Anderson, P., Budden, R. T., Keith, S. B., and Kiven, C. W., 1975, Origin of lineation in the Catalina-Rincon-Tortolita gneiss complex, Arizona (abs.): Geol. Soc. America Abstracts with Programs, no. 7, p. 602.
- _____, Eliopoulos, G. J., Frost, E. G., Goodmundson, R. C., Knapp, R. B., Liming, R. B., Swan, M. M., and Wynn, J. C., 1974, Recumbent folds—focus of an investigative workshop in tectonics: Jour. Geol. Education, v. 22, p. 204-208.
- de Sitter, L. U., 1954, Gravitational tectonics, an essay on comparative structural geology: Am. Jour. Sci., v. 252, p. 321-344.
- Donath, F. A., and Parker, R. G., 1964, Folds and folding: Geol. Soc. America Bull., v. 75, p. 45-62.
- Drewes, Harald, 1976, Laramide tectonics from Paradise to Hells Gate, southeastern Arizona: Ariz. Geol. Soc. Dig., v. 10, p. 151-167.
- Eardley, A. J., 1949, Paleotectonic and paleogeologic maps of central and western North America: Am. Assoc. Petrol. Geologists, v. 33, p. 655-682.
- Fleuty, M. J., 1964, The description of folds: Proc. Geol. Assoc. Engl., v. 75, p. 461-492.
- Harrison, J. V., and Falcon, N. L., 1936, Gravity collapse structures and mountain ranges as exemplified in southwestern Iran: Geol. Soc. London Quart. Jour., v. 92, p. 91-102.
- Hayes, P. T., and Drewes, Harald, 1968, Mesozoic volcanic and sedimentary rocks of southeastern Arizona: Ariz. Geol. Soc. Guidebook III, p. 49-58.
- Jemmet, J. P., 1966, Geology of the northern Plomosa Mountain Range, Yuma County, Arizona (M.S. thesis): Tucson, Univ. of Arizona, 128 p.
- McClymonds, N. E., 1959, Paleozoic stratigraphy of the Waterman Mountains, Pima County, Arizona: Ariz. Geol. Soc. Guidebook II, p. 67-76.
- McKee, E. D., 1934, The Coconino Sandstone—its history and origin: Carnegie Inst. Wash. Pub. 440, p. 77-115.
- _____, 1938, The environment and history of the Toroweap and Kaibab formations of northern Arizona and southern Utah: Carnegie Inst. Wash. Pub. 492, 268 p.
- _____, 1945, Cambrian history of the Grand Canyon region: Carnegie Inst. Wash. Pub. 563, 168 p.
- _____, 1951, Sedimentary basins of Arizona and adjoining areas: Geol. Soc. America Bull., v. 62, p. 481-506.
- _____, 1954, Stratigraphy and history of the Moenkopi Formation of Triassic age: Geol. Soc. America Mem. 61, 133 p.
- _____, 1958, The Redwall Limestone: New Mexico Geol. Soc. Guidebook 9th Field Conf., p. 74-77.
- _____, 1975, The Supai Group—subdivision and nomenclature: U. S. Geol. Survey Bull. 1395J, 11 p.

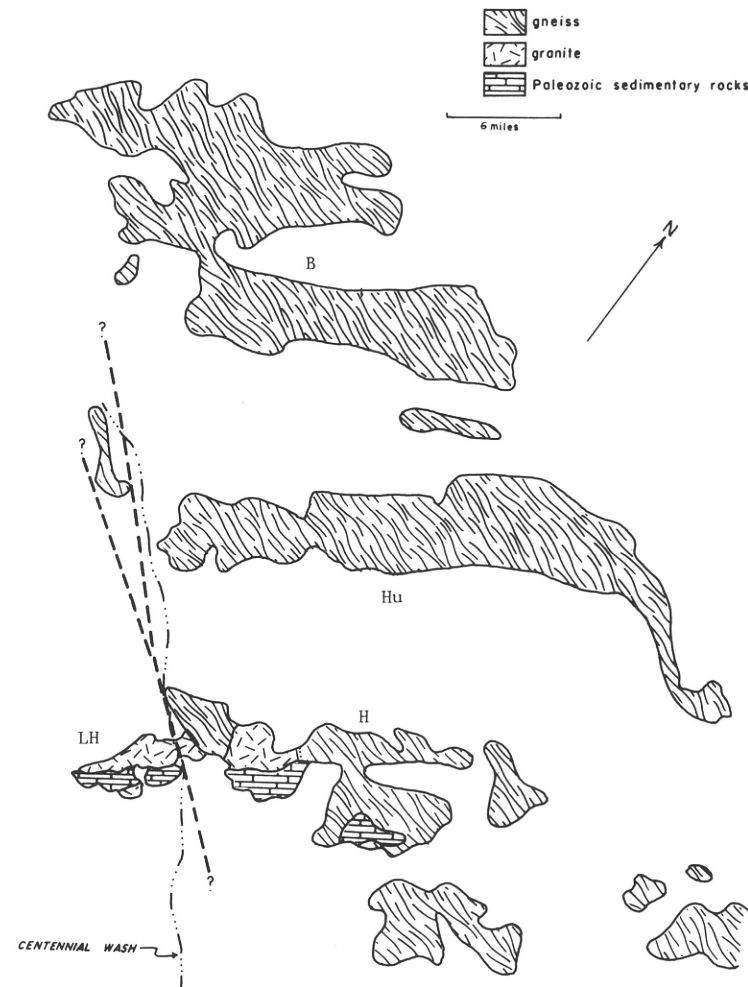


Figure 14. Proposed fault location. Dashed lines are possible locations of a right-handed, reverse-slip fault. Note apparent right-lateral offset of granite-Paleozoic sedimentary rock contact between the Harquahala Mountains and Little Harquahala Mountains. H = Harquahala Mountains, LH = Little Harquahala Mountains, Hu = Harcuvar Mountains, B = Buckskin Mountains.

may also have dipped at a low angle ($\approx 20^{\circ}$ – 30°) to the southeast prior to granite intrusion.

The above relationships in the Harquahala Mountains bear a strong resemblance to the so-called "metamorphic core complexes" of western North America. Characteristic of these terrains is the presence of lineated, low-dipping, cataclastic foliation in gneiss (Coney, in press) which is often overlain by a little-metamorphosed cover sequence deformed by flexural-slip folding and other brittle processes (Armstrong and Hansen, 1966).

Existence of "metamorphic core complexes" is widespread in the western United States. These complexes occur as discrete ranges in a belt from southeastern Arizona (Davis, 1975; Davis and others, 1975) through the eastern Great Basin (Armstrong and Hansen, 1966), and northward into British Columbia (Campbell, 1970; Reesor, 1970). Burchfiel and Davis (1975) feel that they represent exposed culminations of a metamorphic belt which is continuous at depth.

Relative time of formation and uplift of gneiss and gravity gliding in the Paleozoic and Mesozoic sedimentary sequence is difficult to evaluate due to lack of radiometric dating and mapping in western Arizona. Coney (in press) has recognized that south of the Snake River Plain the metamorphic core complexes were "either perpetuated, reactivated, or initiated in Oligocene-Miocene time." This recognition of a possible complex history of core complexes in the southwestern U. S. bears directly on the present problem. Was gravitational tectonics in the sedimentary domain in the Harquahala Mountains concomitant with formation and uplift of a metamorphic core complex or was this deformation merely the result of simple gravity gliding during uplift of a previously formed, rigid core complex? The answer to this question remains largely unanswerable from data presented in this study. Isotopic dating by future workers in western Arizona will aid in establishing age relationships more definitely.

CONTENTS

	page		page
Introduction	1	Bolsa Quartzite	10
Stratigraphy	1	Moenkopi Formation	11
Crystalline Rocks	1	Discussion	12
Gneiss	1	Structural Geology	12
Socorro Granite	3	Structures in Sedimentary Rocks	12
Dike Rocks	3	Socorro Block	12
Sedimentary Rocks	3	Hidden Treasure Block	15
Bolsa Quartzite	6	Structures in Crystalline Rocks	15
Redwall Limestone	6	Structural Evolution	16
Supai Formation	6	Events Recorded in Sedimentary Rocks	16
Coconino Sandstone	7	B ₁ Deformation	16
Kaibab Limestone	7	B ₂ Deformation	17
Moenkopi Formation (?)	7	Gneiss-Socorro Granite Relationships	17
Correlation of Sedimentary Units	8	Gneiss-Gravity Gliding Relationships	17
Kaibab Limestone, Coconino Sandstone,	9	Summary	19
Supai Formation	9	References cited	19
Redwall Limestone	9		

FIGURES

	page		page
1. Generalized geologic map of west-central Arizona (after Wilson, 1960).	2	7. Large-scale crossbedding in Coconino Sandstone.	8
2. Western Harquahala Mountains. View is to the northeast toward Socorro Block.	3	8. Macroscopic fold in Kaibab Limestone.	9
3. Geologic map and sections of a portion of the western Harquahala Mountains, Arizona.	3	9. Total Paleozoic isopach map of Arizona.	10
4. Biotite augen gneiss.	6	10. Comparison of selected Paleozoic sections in Arizona.	11
5. Bolsa Quartzite/Socorro Granite intrusive contact.	7	11. Recumbent folds.	13
6. Cascade fold in Supai Formation.	8	12. Structural stereogram of a layer within the Supai Formation.	14
		13. B ₁ structures.	15
		14. Proposed fault location.	18

Granite intrusion. Socorro Granite definitely intrudes Bolsa Quartzite, the basal unit of the folded sequence. However, it is difficult to determine if granite intrudes, at depth, the large-scale folds and thus postdates their formation or if intrusion and uplift *caused* folding. Figure 5 shows the irregular trace of the granite-Bolsa Quartzite intrusive contact. At this locality, bedding and a large fold in the Bolsa Quartzite were truncated by granite intrusion. This relationship supports a post-B₁ folding time for granite emplacement. Other direct evidence which helps support this hypothesis comes from a small granite dike which crops out in the southwest corner of section 29 (fig. 3). This 90-m-thick dike is similar in mineralogy to Socorro Granite and cuts the Kaibab Limestone "slip sheet." If this dike is indeed equivalent to Socorro Granite, then it follows that intrusion of the Socorro Granite places minimum age constraints on B₁ deformation.

B₂ Deformation

S-shaped flexuring of B₁ trends in the eastern Socorro Block was caused by drag during oblique, right-lateral and reverse movement on the Hidden Treasure Fault. Folds in the Kaibab Limestone slip sheet mentioned above demonstrate this relationship. Northeast-trending fold axes in the sheet are dragged to more easterly trends adjacent to the inferred trace of Hidden Treasure Fault. The near-vertical rotational axis (B₂) and axial plane derived for this flexuring (Varga, 1976) are consistent with a major component of strike-slip motion during faulting. Time of faulting is post-Socorro Granite intrusion because it offsets the granite-Bolsa Quartzite contact.

Flexuring of B₁ trends to a more eastward orientation in the western Socorro Block is not related to any fault known in the study area. Possible placement of a right-lateral fault to account for this flexuring is between the Harquahala Mountains and Little Harquahala Mountains along the present trend of Centennial Wash (fig. 14). The position of this proposed fault is coincident with a major lineament as defined on ERTS imagery of western Arizona. Such a placement is compelling due to the truncation of Precambrian(?) gneissic terrains and apparent right-lateral drag of the western Harquahala Mountains.

Time of northwest-trending, right-handed oblique slip faulting can be inferred from relationships found in the Plomosa Mountains which lie 50 km to the west of the Harquahala Mountains (fig. 1). There, northwest-trending faults which have apparent right-lateral separation cut a post-middle Miocene rhyodacite unit (Miller and McKee, 1971). These faults correspond in time to the beginning of Basin-and-Range extension faulting. Jemmet (1966) also suggests that similar faults in the northern Plomosa Mountains can be assigned to the Basin-and-Range event. The writer extends this reasoning to the Harquahala Mountains and assigns a Cenozoic age (probable post-middle Miocene) to the northwest-trending faults.

EVENTS RECORDED IN CRYSTALLINE ROCKS

It has thus far been established that intrusion of Socorro Granite postdates gravity gliding in the sedimentary domain. It is more difficult to determine, however, the relative timing of development of foliation in gneiss with respect to Socorro Granite intrusion and B₁ deformation.

Gneiss-Socorro Granite Relationships

It is possible that gneissification was syn- or pre-Socorro Granite intrusion. However, if granite intrusion *caused* the gneissic foliation to develop, then a decrease in intensity of gneissification away from the intrusive contact should be observed. Instead, a decrease in foliation development is observed *towards* the contact which is probably the result of recrystallization in the gneiss due to granite intrusion. The writer thus favors the interpretation that intrusion of Socorro Granite postdates development of foliation in gneiss.

A post-gneissification time of granite intrusion is supported by the general concordancy of the granite-gneiss contact to gneissic foliation. This north-northwest-trending contact (fig. 3) is fairly sharp except where granite locally intrudes gneiss in a lit-par-lit fashion. General parallelism of the granite-gneiss contact with foliation orientations in the gneiss indicates that foliation may have provided an inherent weakness along which Socorro Granite was emplaced. Therefore, Socorro Granite in the map area is envisioned as a sill-like body which intruded along the gneiss-Bolsa Quartzite interface. Intrusion thus had the effect of wedging apart the sedimentary rocks from gneiss. Joints in Socorro Granite probably formed as the result of this emplacement. Local development of an incipient foliation parallel to joint surfaces supports this contention.

Gneiss-Gravity Gliding Relationships

The above interpretation implies that rocks of the sedimentary domain were in contact with gneiss during gravity gliding and associated B₁ deformation. Contact relationships 5 km to the west, in the Hercules Mine area, support this suggestion. There, Bolsa Quartzite overlies a 3 m thick schist unit which, in turn, rests directly on gneiss. Bedding in the quartzite and foliation in the schist is concordant to foliation in the underlying gneiss. The dip of the entire sequence is 20°SE.

Based on the above contact relationships it is suggested that the gneiss-Paleozoic sedimentary rock interface was the surface of detachment, or "decollement," during gravity gliding. This zone of decollement served to separate rocks of widely dissimilar metamorphic grade and structural style during deformation. The nature and attitude of this zone cannot be determined due to intrusion of Socorro Granite. However, the low dip of the gneiss-schist-Bolsa Quartzite contact in the Hercules Mine area, and the overall low foliation dips of gneiss in the main Harquahala Mountain mass suggests that the zone of decollement in the study area

foliation planes vary from 16°NW. in the extreme western part of the map area to 80°NE. near the granite-gneiss contact. Mineral lineation on the foliation plane, where present, trends approximately N.5°W. and plunges at shallow angles to the northwest or northeast. Strike of the foliation plane is constant throughout the exposure of gneiss except where rotated by a N.60°W. striking fault (fig. 3).

Pervasive, closely spaced joints are the dominant planar elements in Socorro Granite (fig. 3). Spacing of joints is as close as 2 cm at some localities. The average orientation of joints is N.8°W. in strike and vertical in dip. Orientation of joints is approximately parallel to the granite-gneiss intrusive contact and to foliation within the gneiss. Locally, joint orientations in the granite are also parallel to the trend of the granite-Bolsa Quartzite intrusive contact. In the Socorro Mine area (fig. 3), near this contact, joints grade into a faint, incipient foliation defined by slight alignment of mica and feldspar crystals. A similar incipient foliation is observed in the center of the Socorro Granite exposure near the middle of section 23 (fig. 3).

Diabase dikes have intruded the crystalline domain both parallel and transverse to foliation and joints. Quartz dikes are also parallel to foliation and joints, and possess a pervasive jointing which reflects this parallelism.

STRUCTURAL EVOLUTION

Formation of "cascade" folds (B_1 folds) and their subsequent s-shaped flexuring (B_2 folds) record two distinct periods of deformation in the Paleozoic-Mesozoic sedimentary sequence (Varga, 1977). Insights into the structural evolution of the Harquahala Mountains can be gained through an understanding of the origin and relative timing of these two fold events in relation to formation of the gneiss and granite crystalline complex. Absolute timing of such events can only be inferred due to lack of radiometric dating in the region. An attempt will be made to correlate structural events in the western Harquahala Mountains to those of other mountain ranges which have similar structural sequences.

EVENTS RECORDED IN SEDIMENTARY ROCKS

B_1 Deformation

The presence of abundant bedding-plane faults (fig. 3) suggests an initial period of low-angle tectonic transport within the rocks of the sedimentary domain. Bedding-plane faulting has cut out several hundred meters of section between certain formations. The most notable of such faults occurs in the Hidden Treasure Block at the base of the Coconino Sandstone. Successive formations are cut out beneath the Coconino Sandstone until it rests directly on folded Bolsa Quartzite. The upper, cherty marble unit of the Redwall Limestone is cut out to varying degrees beneath the Supai Formation throughout the sedimentary domain. Bedding-plane movements are believed to have occurred prior to, as well as concomitantly with B_1 folding.

Such a model permits the associated occurrence of folded bedding-plane faults as well as those which truncate folds.

Several features associated with this initial period of presumed low-angle tectonic transport suggest that deformation occurred as the response to body, or gravitational, forces as opposed to lateral compressional forces. Bedding-plane faults in the sedimentary domain primarily place younger strata on older strata. Armstrong (1972) has suggested that such "younger on older" or denudation faults are almost certainly of gravitational origin. B_1 folds possess several morphologic features which are also indicative of a purely gravitational origin. Presence of unthinned and unfaulted reversed limbs of large folds is thought by de Sitter (1954, p. 337) to be "strong evidence for gravity tectonics." Reversed limbs are a common feature of B_1 folds (see cross sections A-A', B-B', C-C' and fig. 12). "Cascade" morphology of folds, as seen in figure 12, is also strong evidence for deformation predominantly under gravitational forces (Harrison and Falcon, 1936).

Fold analysis (Varga, 1976) restricts the movement direction within the sedimentary rocks during B_1 deformation to a N.39°W./S.39°E. line. However, inspection of the entire fold system in cross section A-A', B-B', C-C', and figure 12 reveals a general overturning of folds to the southeast. It is concluded, therefore, that tectonic transport accompanying gravity gliding was S.39°E. Several faults and their associated minor structures which formed during gravitational gliding support this sense of transport.

The reverse fault in the southern portion of the Hidden Treasure Block is thought to have formed during gravity gliding. This fault brings folded Coconino Sandstone over an anticline composed of Kaibab Limestone and cored by Coconino Sandstone. Minor folds associated with this fault verge to the south-southeast, a direction consistent with the southeast-directed tectonic transport derived for B_1 folds. Overriding of Coconino Sandstone along this fault was possibly a response to local compression due to crowding at the toe of the glide sheet.

The slab of folded Kaibab Limestone which overlies Moenkopi Formation(?) in fault contact in the southwest corner of section 29, was also emplaced during gravity gliding. Minor reverse faults at the fault contact indicate movement to the southeast. Northeast axial trends of folds within the slab are consistent with this movement direction. Emplacement of the Kaibab Limestone slab is envisioned to have occurred in a mode similar to formation of a "slip sheet" (Harrison and Falcon, 1936, p. 93). A slip sheet, in this sense, is a slab which slides down the steepening flank of an anticline and overrides strata of a younger age. A possible source of the Kaibab Limestone slab is the large recumbent fold immediately to the northwest. Also thought to be a slip sheet is the small slab of Redwall Limestone in the northwest corner of section 20 (fig. 3).

Timing of gravity gliding is clearly post-Moenkopi Formation(?) deposition (Triassic) and possibly pre-Socorro

GEOLOGY OF THE SOCORRO PEAK AREA, WESTERN HARQUAHALA MOUNTAINS

by
Robert J. Varga

Arizona Bureau of Mines*

INTRODUCTION

The west-central and southwestern portions of Arizona have remained a geologic enigma since the pioneering mapping in the region by Eldred Wilson of the Arizona Bureau of Mines. Until recently, such factors as adverse weather conditions, remoteness of terrain, and relative lack of known, large, economic mineral deposits have discouraged subsequent, more detailed investigations of this area. Hence, an impressive amount of information concerning the geology of the more populous parts of the state continued to grow while western Arizona remained in relative "geologic infancy." This imbalance of understanding has become increasingly obvious as models have been developed depicting the regional tectonic and stratigraphic development of Arizona. Fortunately, in the last decade these "gaps" in our models have stimulated geologists to greater activity in the western portion of the state.

It is now generally believed by those working with the regional geologic framework of Arizona that an understanding of this part of the Basin-and-Range Province is critical to the evaluation of proposed extensions of Cordilleran tectonic and stratigraphic trends into southeastern Arizona. The northeast-trending Harquahala Mountains lie within this critical terrain and display relationships which may aid in defining the nature of any stratigraphic or tectonic linkage through this area. The present study deals with the geology of the Socorro Peak area in the western Harquahala Mountains.

The Harquahala Mountains lie, physiographically, within what is generally considered to be the Transverse Range region of the Basin-and-Range Province (Wilson and Moore, 1959). The general geology of this part of Arizona, shown in figure 1, is taken largely from the Geologic Map of Yuma County (scale 1:375,000) by Wilson (1960). The only other geologic mapping which has been done to date in this part of western Arizona has been by Miller (1966, 1970) and Jemmet (1966) in the Plomosa Mountains, Shackelford (1975) in the Rawhide Mountains,

*This study represents work completed in 1975-76 while the writer was a graduate student at the University of Arizona and a Graduate Research Assistant for the Arizona Bureau of Mines (now the Bureau of Geology and Mineral Technology).

Blanchard (1913) in the Buckskin Mountains, and Ciancanelli (1965) in the Granite Wash Mountains.

In general, the geology of west-central Arizona is dominated by an abundance of Mesozoic and Cenozoic volcanics, intrusives, and sediments and Precambrian (?) gneiss with subordinate Paleozoic sediments.

The Harquahala Mountains are composed dominantly of gneiss, schist, and granite with two overlying masses of Paleozoic and Mesozoic sediments (fig. 2). The contact between these sedimentary blocks and the underlying crystalline terrain was interpreted as a thrust fault by Wilson (1960, 1962). The northeast trend of the Harquahala Mountains is generally parallel to the Harcuvar and southern Buckskin ranges to the north but is otherwise discordant to the dominant northwest trend of the region.

STRATIGRAPHY

With the exception of the schist terrain shown on the generalized geologic map (fig. 1), the study area includes all of the major rock types found in the Harquahala Mountains. These include gneiss, granite, diabase dikes, and Paleozoic and Mesozoic sedimentary rocks.

CRYSTALLINE ROCKS

Gneiss

The rocks termed collectively "gneiss" in this circular are dominantly biotite augen gneiss with minor biotite gneiss and quartz-mica schist. These gneissic rocks are only exposed east of Tenahatchapi Road (fig. 3); in the map area, however, they make up the larger portion of the Harquahala Mountains.

Biotite augen gneiss is the dominant rock type in this unit (fig. 4). Reconnaissance suggests that it also comprises a large portion of the main Harquahala Mountain mass mapped as Precambrian gneiss (fig. 1). The biotite augen gneiss is composed of white potassium feldspar augen, or porphyroclasts, which lie within a foliated matrix of biotite, quartz, and feldspar in approximately equal proportions. The augen, which vary in size up to 3 cm in length, are lensoidal to tabular in shape and comprise about 40 percent of the total rock volume. The long axes of these augen define a poorly developed lineation within the foliation plane.

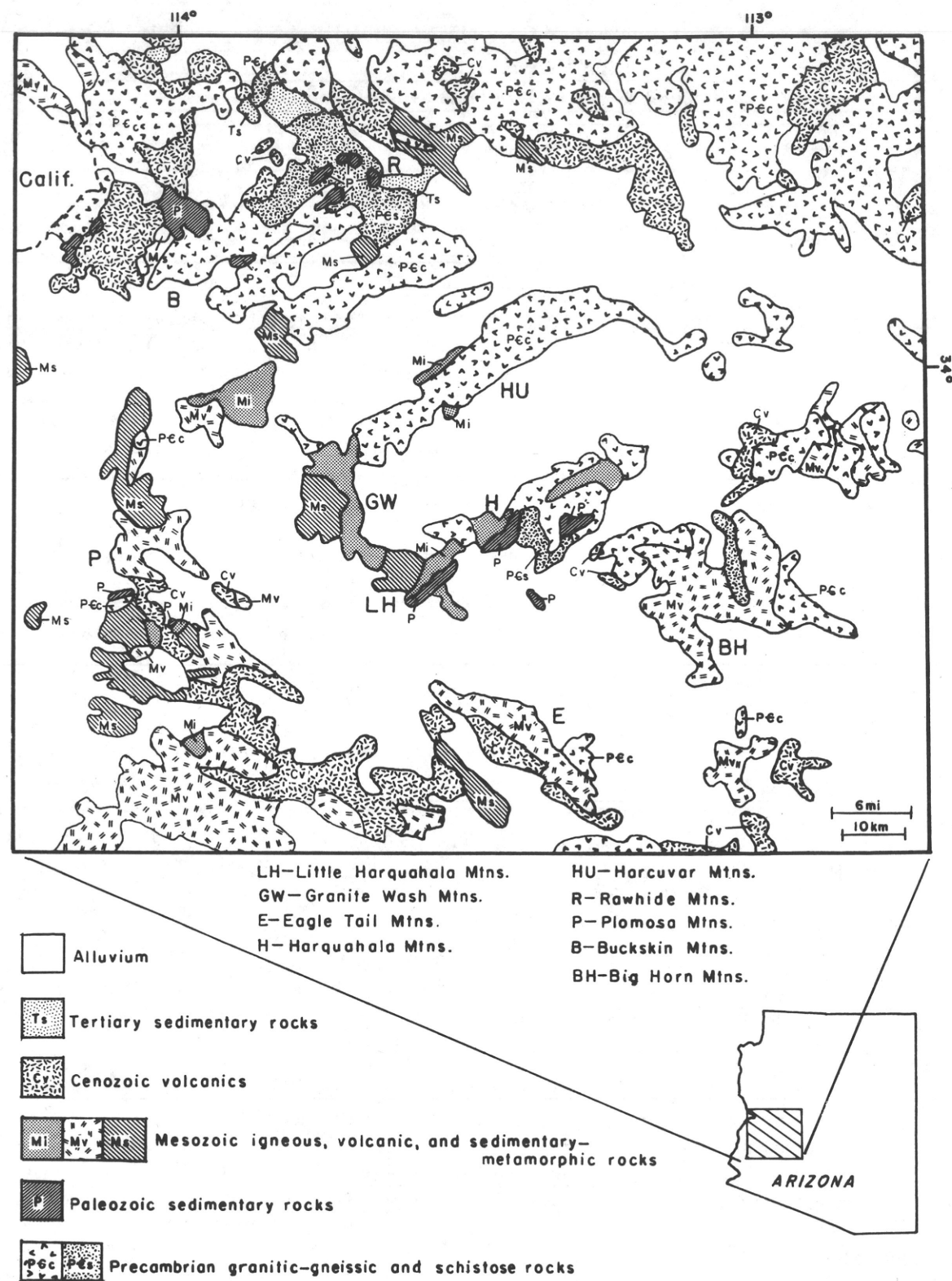


Figure 1. Generalized geologic map of west-central Arizona (after Wilson, 1960).



Figure 13. B, structures. View to the southeast, towards Hidden Treasure Block. Note highly folded Coconino Sandstone.

Hidden Treasure Block

The Hidden Treasure Block is separated from the Socorro Block by the Hidden Treasure Fault (fig. 3). This fault has a slightly curvilinear trace which varies from N.35°W. at its southern end to N.20°W. in the northern part of the area. Dips on the fault are at very high angles (75°–86°) to the northeast.

Movements on the Hidden Treasure Fault postdate large-scale, recumbent folding in the sedimentary domain. Near the postulated southern extension of this fault under alluvium, fold axes in Kaibab Limestone appear to be dragged in a right-lateral sense. Offsets of formational contacts across the fault also reveal right-lateral separation. In the northeastern corner of section 30, offsets and drag of strata suggest reverse movement on the Hidden Treasure Fault such that the Hidden Treasure Block has moved up relative to the Socorro Block. Where the fault cuts Bolsa Quartzite in the northern part of the area, slickensided surfaces are locally developed. The slickensides plunge at low angles (12°–35°) to the southeast and, coupled with the above separation data, suggest relative normal-slip on the fault at this locality. This suggested normal-slip is contrary to the observed reverse-slip offsets. This complication may be due to local movements on the several fault splays which diverge from the main Hidden Treasure Fault trace in this area. Right-handed reverse-slip is suggested as the dominant sense of displacement on the Hidden Treasure Fault. The relative amounts of strike-slip versus reverse-slip cannot be determined due to lack of slickenside data along most of the fault trace.

The structure of the Hidden Treasure Block can be observed in cross section D–D' (fig. 3). Folds in the block have similar physical attributes as do those in the Socorro Block. Axes of all folds measured plunge at shallow to

moderate angles dominantly to the east-northeast, about an average trend of N.68°E. Axial surfaces of these folds dominantly dip steeply to the north. Thus, folds in the Hidden Treasure Block can be characterized as gently plunging and steeply inclined (Fleuty, 1964) in contrast to the more recumbent folds of the Socorro Block.

The relationship of structures in the Hidden Treasure Block is summarized in cross section D–D'. Macroscopically folded Bolsa Quartzite, Redwall Limestone, and Supai Formation are truncated and overridden by Coconino Sandstone beneath a southeast-dipping, sub-bedding-plane fault. At some localities this fault is defined by a gouge zone up to 65 cm in thickness. Where observed at other localities, the fault appears to be a "knife-edge" contact with no well defined breccia or gouge zone. Coconino Sandstone above this flat fault is little deformed but becomes highly folded towards the south where it overrides a large, southeast-plunging anticline along a high-angle fault (fig. 13). Minor folds associated with the reverse fault are asymmetric and verge to the southeast. Another fault in this system juxtaposes a small slab of Redwall Limestone over Coconino Sandstone in the northwest corner of section 20. This fault plane has been intruded by diabase dikes.

Post-folding, high-angle faults which cut the southern part of the Hidden Treasure Block are similar in trend to the Hidden Treasure Fault. Where exposed, these faults indicate normal separation, although a component of strike-slip separation cannot be ruled out.

STRUCTURES IN CRYSTALLINE ROCKS

Foliation and joints are the dominant structures within the crystalline domain (fig. 3). Gneiss, which makes up the western part of the domain, contains a northwest-striking foliation with an average orientation of N.10°W. Dips of

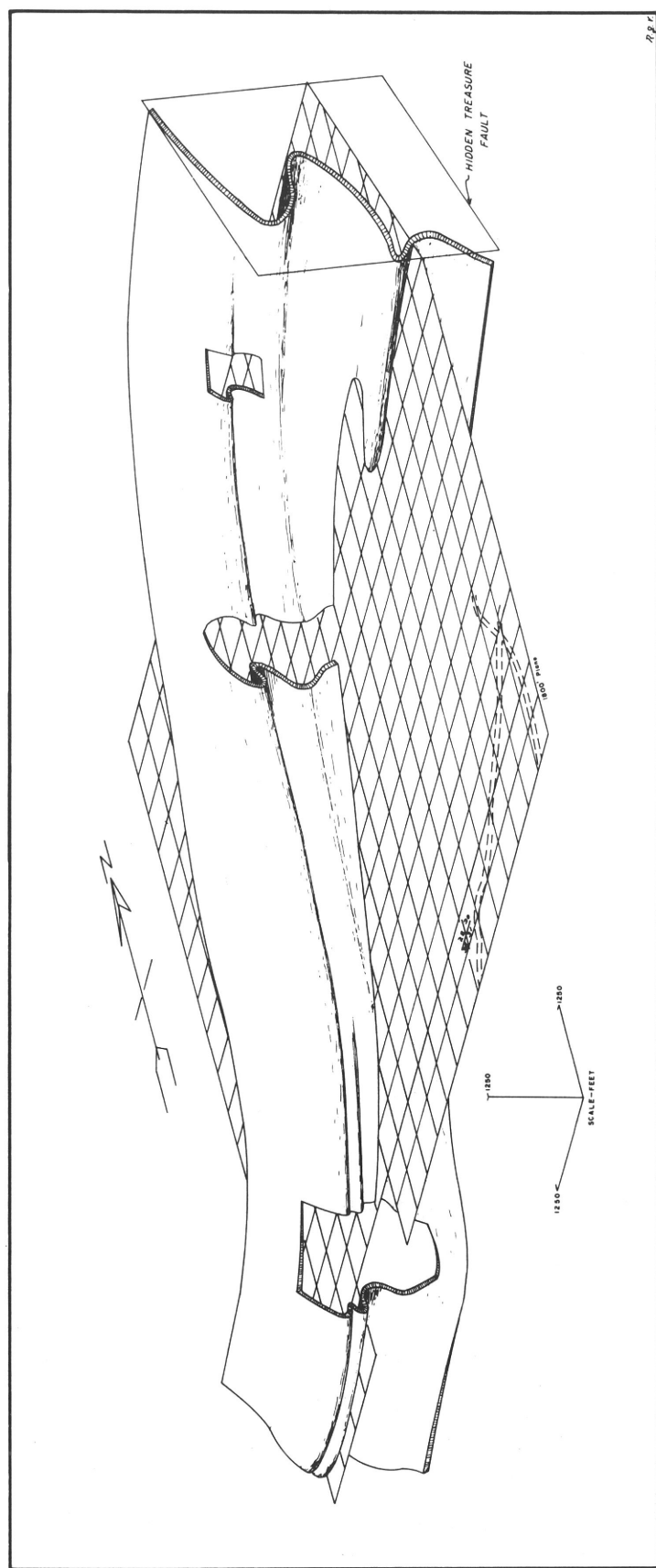


Figure 12. Structural Stereogram of a layer within the Supai formation.



Figure 2. Western Harquahala Mountains. View is to the northeast toward Socorro Block. Lithologic contacts shown are: gr = Socorro Granite, B = Bolsa Quartzite, R = Redwall Limestone, S = Supai Formation, C = Coconino Sandstone, and K = Kaibab Limestone.

Variably interlayered within the biotite augen gneiss are minor quartz-mica schist and biotite gneiss. A faint mineral lineation is observed on foliation surfaces of these rocks which is parallel in orientation to the lineation within the adjacent biotite augen gneiss.

Socorro Granite

A large quartz monzonite to granite body, herein referred to informally and collectively as the Socorro Granite, forms a topographically subdued terrain between the gneissic rocks to the west and the sedimentary sequence to the southeast (fig. 2).

The dominant composition of the Socorro Granite lies well within the granite field as defined by Streckeisen (1973). Typically, this medium-grained, equigranular rock is composed of approximately 45 percent quartz, 32 percent microcline, 20 percent sericitized plagioclase and 3 percent muscovite mica. Minor amounts of hornblende and biotite mica are locally present.

The Socorro Granite intrudes into both the overlying sedimentary sequence and the gneiss. The granite intrudes the gneiss concordantly as is evidenced, at map scale (fig. 3), by the general parallelism of the contact with the trend of gneissic foliation.

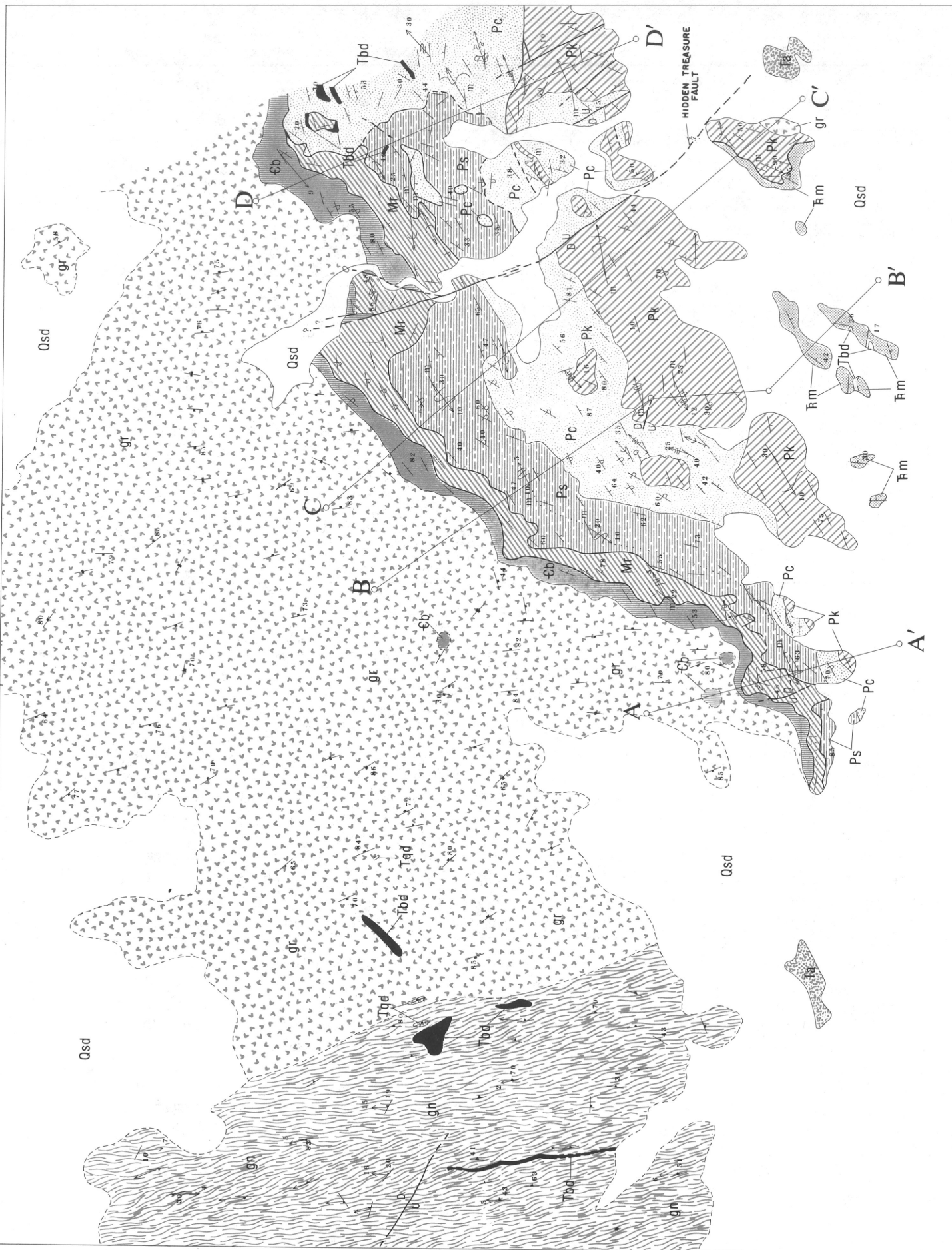
Dike Rocks

Hornblende diabase dikes, which vary up to 120 m in thickness, cut all rocks in the map area (fig. 3). The dike rocks are composed of fine-grained plagioclase and hornblende which together display a diabasic texture. The hornblende in these dikes is locally altered to epidote.

Quartz dikes, up to 10 m thick, cut gneiss and Socorro Granite. Unaltered rhyolitic dikes are also present but the intrusive relationship of these dikes to the other rock types in the study area is unclear. This is because where the rhyolite dikes are exposed, they are surrounded by recent alluvium. Rhyolite dikes are up to 170 m thick.

SEDIMENTARY ROCKS

A thick sequence of Paleozoic and Mesozoic sedimentary rocks is exposed in the southeastern portion of the study area. These rocks continue in outcrop farther to the east of the mapped area and are also exposed in the easternmost sedimentary block shown in figure 3. In the study area, these sedimentary rocks are deformed into large-scale folds. The folding, and associated deformation, makes thickness estimations of the various formations difficult. The thicknesses given below should be interpreted as an extreme upper limit, as the tendency is to overestimate stratigraphic thickness in folded terrains.



A



B

Figure 11. Recumbent folds. (A) Macroscopic fold in Kaibab Limestone. View is to the SE. Sense of overturning of fold is to the SE. (B) Mesoscopic fold in Coconino Sandstone.

sins and are not recognized very far north of Tucson, Arizona (Hayes and Drewes, 1968).

The clastic unit which overlies Kaibab Limestone in the study area is, therefore, provisionally assigned the name Moenkopi Formation(?). It is hoped that stratigraphic studies by future workers in west-central Arizona will further test the validity of such a correlation.

Discussion

The preceding correlations confirm the existence of a considerable section of Paleozoic rocks in the Harquahala Mountain area as mentioned briefly by McKee (1951) and by Wilson (1962). The total Paleozoic section estimated in the study area is approximately 1,258 m. This estimated figure should be interpreted as an extreme maximum thickness. Miller (1970) reports approximately 853 m of Paleozoic strata in the Plomosa Mountains. These thicknesses are shown plotted on McKee's (1951) total Paleozoic isopach map of Arizona shown here as figure 9. It is evident that the positions of the 2,000 ft, 3,000 ft, and 4,000 ft contours in western Arizona should be displaced to the southwest since the position of the contour lines in west-central Arizona was originally based on thickness estimates in these two mountain ranges (McKee, 1951).

Tentative correlation of the post-Kaibab clastic rocks with Triassic Moenkopi Formation supports the original contention by McKee (1954) that the Moenkopi Formation once continued south of its previously recognized southern limit in the Mogollon Rim area and that it has largely been removed by pre-Cretaceous erosion.

STRUCTURAL GEOLOGY

The most conspicuous structural features in the western Harquahala Mountains are large-scale folds which pervade the Paleozoic-Mesozoic sedimentary rocks. Associated with these folds are abundant bedding plane faults. In contrast, rocks of the underlying crystalline complex are not generally folded or faulted but contain other well-developed features such as joints, foliation and mineral lineation. The following discussion presents a general description and interpretation of these various structures and attempts to relate them to a structural sequence which, hopefully, will characterize a part of the geologic history of this complex area of western Arizona. A more rigorous, analytical treatment of the structures described herein is presented elsewhere (Varga, 1976).

STRUCTURES IN SEDIMENTARY ROCKS

The Paleozoic-Mesozoic sedimentary sequence can be divided into two domains based on contrasting structural style. The Hidden Treasure Fault serves to separate the two domains which are referred to below as the Socorro Block and the Hidden Treasure Block (fig. 3). In general, the

Socorro Block is dominated by large-scale, recumbent folding, whereas the Hidden Treasure Block is characterized by upright, large-scale folding. High-angle and bedding-plane faults are present in both blocks.

Socorro Block

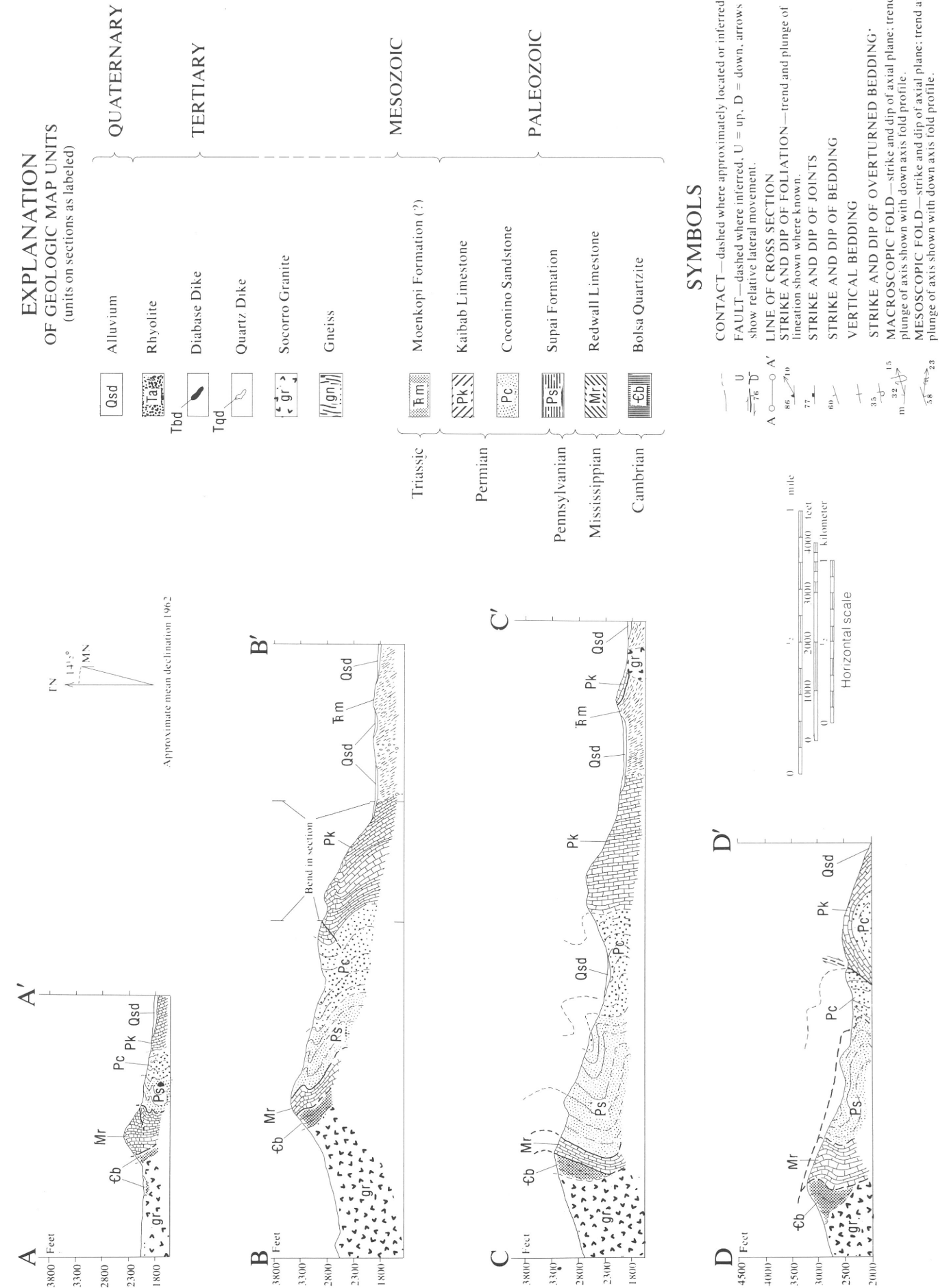
The Socorro Block is a structurally homogeneous terrain characterized by large-scale, subhorizontal, gently inclined to recumbent (Fleuty, 1964) folds as are seen in figures 6, 8, and 11A, and in cross section in figure 3. Geometrically, these large-scale folds are generally concentric in profile with some minor interlayer hinge-zone thickening. Hinge-zone thickening is best developed in the calcareous layers of the Kaibab Limestone (fig. 8) and Redwall Limestone. The large-scale folds can thus be considered as transitional between flexural-slip and flexural-flow (Donath and Parker, 1964). Tightness of folding, as determined by interlimb angle (Fleuty, 1964), varies from close (70° to 30°) to tight ($<30^\circ$). Small-scale folds (fig. 11B) are also present in all rock types in the Socorro Block and display variations in fold style similar to those of large-scale folds.

Axes of all folds measured in the Socorro Block have shallow plunges and vary up to 40° in trend about an average orientation of $N.58^\circ E$. Axial surfaces of folds generally dip gently to the northwest or southeast.

The morphology of overall folding in the Socorro Block is most easily visualized in tracing out a particular layer within the folded sequence. Figure 12 is a structural stereogram of a layer within the middle portion of the Supai Formation. The inferred effects of erosion have been removed in this reconstruction. The overall morphology of this layer is that of vertically stacked, recumbent folds similar to the "piles of folds" described by Davis and others (1974). Such stacks of recumbent folds have been appropriately termed "cascade folds" by Harrison and Falcon (1936).

Also evident in plan view in the structural stereogram, and on the geologic map, is a gentle, s-shaped flexure in the attitude of both bedding and fold axes. In the southwestern part of the Socorro Block, fold axes and bedding follow a nearly east-west trend and turn northeastward in the central portion of the block. In the eastern part of the block, near the Hidden Treasure Fault, fold axes and bedding again turn to the more eastward orientations.

Several high- and low-angle faults are observed in the Socorro Block (fig. 3). Northwest-trending, high-angle faults are of minor extent and indicate normal and reverse movements. A flat fault near the Socorro Mine area offsets the axial portion of a large fold in the Redwall Limestone and places reddish dolomites over quartzites of the Supai Formation. Separation across this fault is up to 25 m. Another low-angle fault in the southeastern portion of the Socorro Block places folded Kaibab Limestone over gently dipping Moenkopi(?) Formation. Minor reverse faults located near this fault contact dip to the northeast.



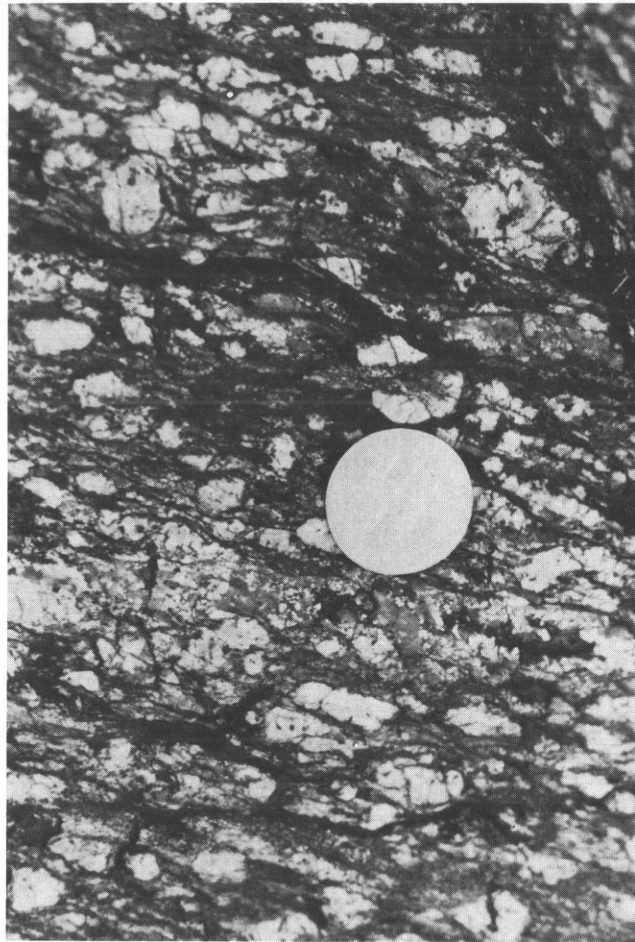


Figure 4. Biotite augen gneiss. Note tabular augen composed of potassium feldspar which lie in a foliated matrix composed dominantly of biotite, feldspar, and quartz.

Correlation of the sedimentary rocks exposed within the Harquahala Mountains to specific formations is hindered due to the paucity of fossils and to the relatively large distances from the study area to locations of stratigraphic sections which have been studied. These difficulties, combined with the observance by McKee (1951) that the Harquahala Mountains lie within an area which separated two active geosynclines during the Paleozoic, make any stratigraphic correlation tenuous.

The rock units are named and described below. Following these descriptions is a discussion which summarizes the basis for correlation of these units to specific formations. The separation of rock description and correlation is made here in the hope that this will facilitate stratigraphic revisions in the future as western Arizona receives more attention and study.

Bolsa Quartzite

In the Harquahala Mountains, the Bolsa Quartzite is a medium-bedded, arkosite composed of poorly sorted, sub-rounded quartz and potassium feldspar fragments. The

quartz fraction comprises about 70 percent of the rock volume while the feldspar fraction totals approximately 30 percent. Color of this formation is typically grayish brown (5YR 3/2) on weathered surfaces and pale brown (5YR 5/2) to grayish purple (5P 4/2) on fresh surfaces. Bolsa Quartzite crops out along the entire length of the sedimentary block and forms a prominent ledge over the more gentle slopes composed of granitic rock (fig. 5). Thickness of the Bolsa Quartzite is up to 106 m, but varies along strike.

The contact of the Bolsa Quartzite with the underlying Socorro Granite is intrusive (fig. 5). Although a chill zone was not observed in the Socorro Granite along this contact, the granite clearly intrudes and locally envelopes portions of the quartzite. Isolated blocks of Bolsa Quartzite occur as inclusions within the granite as is seen in cross-section A-A' (fig. 3). Evidence for slight recrystallization of the Bolsa Quartzite near this contact is evidenced in thin section, by the interlocking nature of many of the quartz and feldspar grain boundaries.

Redwall Limestone

The most distinctive and readily mappable stratigraphic unit in the Harquahala Mountains is the Redwall Limestone (fig. 2). This formation is composed dominantly of very homogeneous, medium- to massive-bedded dolomite. Very little chert was observed within this formation. Color of the dolomite ranges from grayish orange-pink (5YR 7/2) to grayish orange (10YR 7/4) on weathered surfaces and light red (5R 6/6) to grayish pink (5YR 7/2) on fresh surfaces. Locally, an upper unit of the Redwall Limestone is observed. This unit is a thin-bedded, white marble with abundant chert and minor phyllite layers. Thickness of the Redwall Limestone ranges up to 115 m.

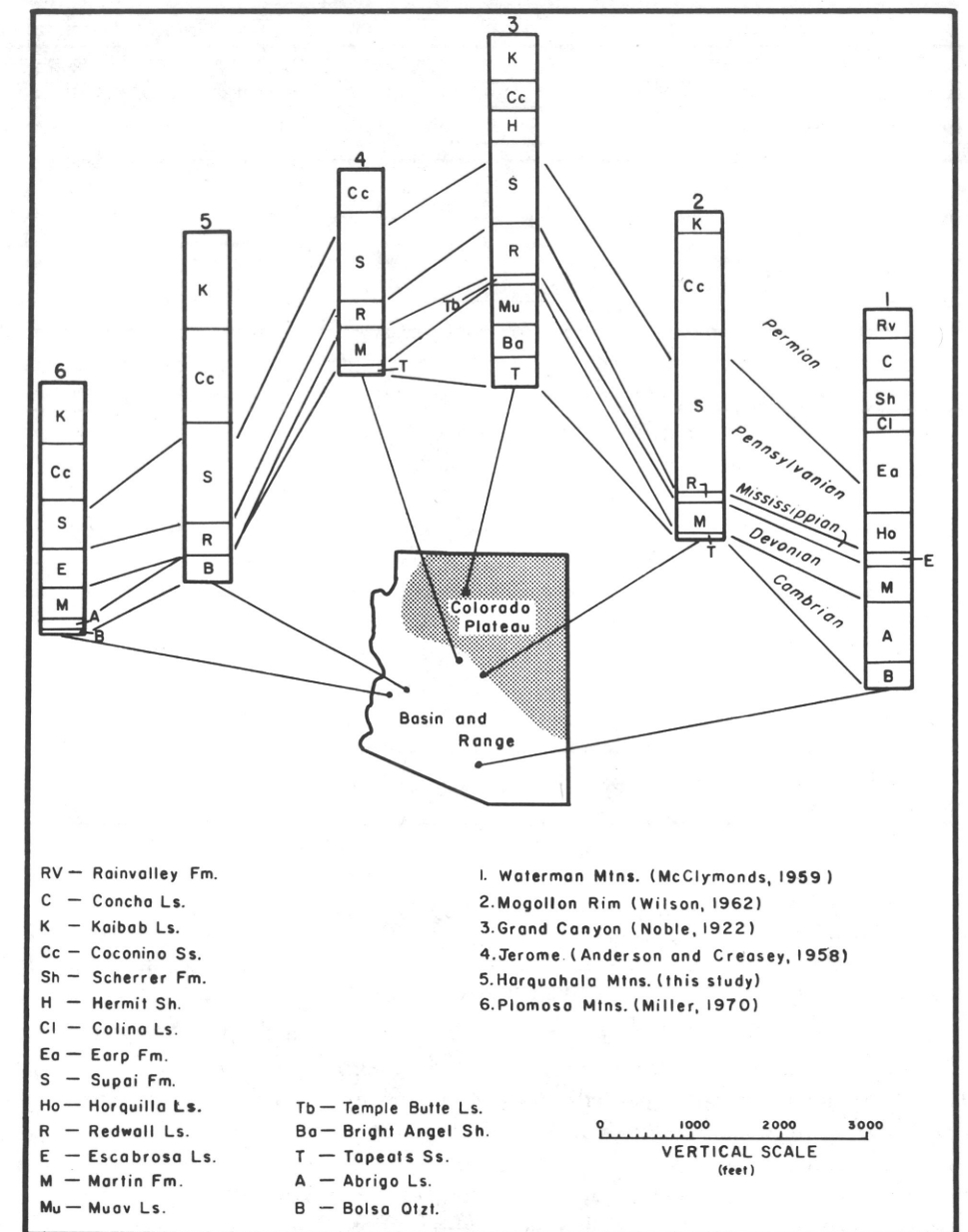
The pink to red dolomitic lower unit of the Redwall Limestone rests in fault contact with underlying Bolsa Quartzite throughout the map area. This fault contact is everywhere defined by a mylonite which was seen to vary in thickness from 3 cm to 3 m. The mylonite is reddish in color and is composed of fine-grained, calcareous material.

Supai Formation

The Supai Formation is a very heterogeneous unit composed dominantly of quartzite interbedded with minor limestone and phyllite layers. This formation is up to 365 m in the study area.

Medium-bedded quartzite comprises most of the Supai Formation (fig. 6). This quartzite is pale red (10R 6/2) on fresh surfaces and light brown (5YR 6/4) on weathered surfaces. Small-scale crossbedding and flaser bedding is locally present in the quartzites. Minor limestone is interbedded with these quartzites throughout the thickness of the Supai Formation. Two main limestone types are present. The most abundant type is a thick-bedded limestone which has a blocky appearance in outcrop. This blocky limestone is pale red (5R 6/2) on fresh surfaces and pale, yellowish

Figure 10. Comparison of selected Paleozoic sections in Arizona. Correlation lines are lines of approximate time equivalence.



change. To the north, along the Mogollon Rim, the Redwall Limestone is underlain by Martin Formation and Cambrian Tapeats Sandstone (fig. 10).

It thus appears that, from stratigraphic sequence considerations, the lowermost quartzite unit in the Harquahala Mountains may tentatively be correlated to either the Tapeats Sandstone or to the Bolsa Quartzite. The Tapeats Sandstone (Noble, 1922; McKee, 1945) in the Colorado Plateau region is described as a massive-bedded, chocolate brown, crossbedded sandstone. The Bolsa Quartzite is typically brown to reddish brown quartzite which becomes more feldspathic in its lower part (Bryant, 1968). The arkosite which forms the base of the sedimentary section in the Harquahala Mountains is lithologically more similar to the lowermost Bolsa Quartzite and is thus correlated with it.

Moenkopi Formation(?)

Overlying the Kaibab Limestone is a unit composed chiefly of quartzite, phyllite and minor conglomerate. The contact between these two units is not observed, however, in the map area. Miller (1966) found a similar sequence of clastic rocks in the Plomosa Mountains and assigned to them a lower Mesozoic(?) age. He further suggests that they may be correlative with the Triassic Moenkopi Formation which overlies the Kaibab Limestone on the Colorado Plateau.

Possible correlatives in the southern Arizona rock record are the lower Mesozoic volcanic and associated sedimentary rocks. The lower Mesozoic strata, consisting of the Canelo Hills Volcanics, Mount Wrightson Formation, and Recreation Redbeds, were apparently deposited in local ba-

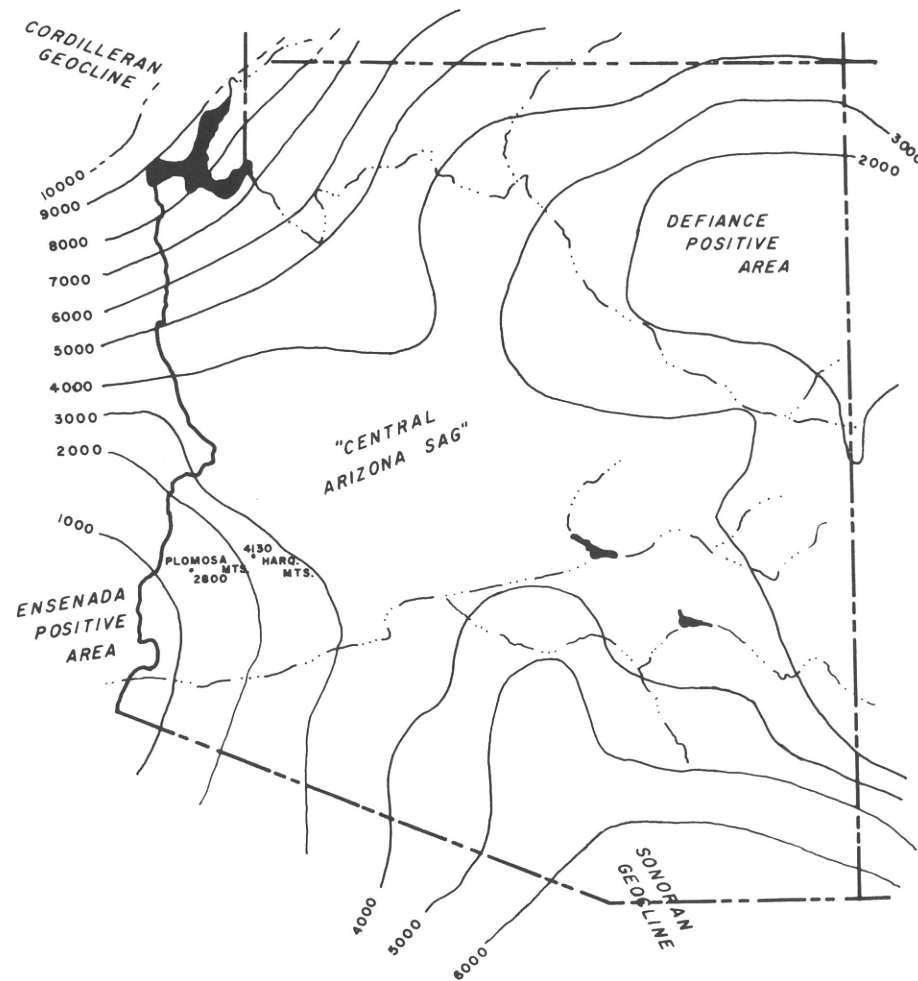


Figure 9. Total Paleozoic isopach map of Arizona. All thickness figures shown are given in feet (after McKee, 1951).

Beneath the Supai Formation on the Colorado Plateau is the Mississippian Redwall Limestone. McKee (1958) describes the bottom member of the Redwall Limestone in the Grand Canyon as pale-red to gray dolomite. Above this member is the relatively thin lower middle member composed of cherty, pale-brown limestone. The pink dolomite unit in the Harquahala Mountains, and its uppermost cherty, white marble layers are correlated with this lowermost part of the Redwall Limestone.

Miller (1970), using fossil evidence, assigned a Mississippian age to similar dolomites and cherty limestones which underlie the Supai Formation in the Plomosa Mountains. He correlated this unit, however, to the massive-bedded, gray-colored Escabrosa Limestone (Bryant, 1968) of southern Arizona (fig. 10). The writer feels that, lithologically, correlation of this unit to the Redwall Limestone is much more satisfactory.

Bolsa Quartzite

Underlying the pink to red dolomites of the Redwall Limestone in the Harquahala Mountains is an arkosite. The contact between these two units is everywhere a bedding-

plane fault. Reconnaissance to the west, in the Little Harquahala Mountains, suggests that a considerable sequence of black to gray, cherty dolomites conformably underlies the pink to red dolomites of the Redwall Limestone. Beneath these black to gray dolomites is a thick-bedded arkosite similar to that found to underlie Redwall Limestone in the study area. Miller (1966, 1970) describes a similar sequence in the Plomosa Mountains. He assigned the black to gray dolomites to the Devonian Martin Formation of southeastern Arizona (Bryant, 1968) and the basal quartzite to the Cambrian Bolsa Quartzite (Bryant, 1968), also a southeastern Arizona stratigraphic unit. Martin Formation is apparently missing in the Harquahala Mountains and its absence may be due to bedding-plane faulting between the Redwall Limestone and the arkosite. In the Plomosa Mountains, Miller (1970) recognized an interbedded shale and quartzite unit between the Bolsa Quartzite and Martin Formation which he correlated with the Cambrian Abrigo Formation of southeastern Arizona. This shale and quartzite unit is not recognized in the Harquahala Mountains nor in the Little Harquahala Mountains, and its absence may be due to erosion, non-deposition, or facies

Figure 5. Bolsa Quartzite-Socorro Granite intrusive contact. View is to the NE. Note irregular trace of contact. Bedding in quartzite is steeply dipping to the NW. Lithologic units shown are: gr = Socorro Granite and B = Bolsa Quartzite.



brown (10YR 6/2) on weathered surfaces. In contrast, a finely laminated limestone was found which is moderate orange-pink (10R 7/4) on fresh surfaces and pale red (10R 6/2) on weathered surfaces. Field recognition of these various rock types within the Supai Formation is hindered by the development of black desert varnish on most exposed surfaces.

The contact of the Supai Formation with underlying Redwall Limestone is a probable fault. At most localities, this contact is marked by a dark green phyllite with well developed cleavage which parallels bedding. The phyllite ranges up to 2 m in thickness. The upper white marble unit of the Redwall Limestone is, in most areas, completely cut out by this fault which brings the Supai Formation into contact with the pink to red dolomites of the lower Redwall Limestone.

Coconino Sandstone

The Coconino Sandstone is a homogeneous, thin-bedded quartzite throughout the Harquahala Mountains. The most distinguishing characteristic of this formation, relative to the quartzites of the Supai Formation, is its homogeneity. Thickness of the Coconino Sandstone in the map area is approximately 335 m. The quartzite is fine-grained and has a vitreous luster and clear to white color on fresh surfaces. The Coconino Sandstone tends to form slopes and saddles between the enclosing Supai Formation and Kaibab Limestone. Small-scale crossbedding is abundant throughout the Coconino Sandstone, and large-scale crossbedding is locally present (fig. 7).

The contact of the Coconino Sandstone with the underlying Supai Formation appears to be conformable and depositional in nature. The reddish quartzites of the Supai

Formation grade upward into, and intertongue with, the more vitreous quartzites of the Coconino Sandstone at this contact.

Kaibab Limestone

Approximately 335 m of varicolored limestone overlies quartzites of the Coconino Sandstone. This formation, the Kaibab Limestone, is divisible into a lower, slope-forming unit and an upper, cliff-forming unit (fig. 8).

The lower unit is composed of medium- to thick-bedded limestone with minor chert lenses. The main distinguishing feature of this lower unit, besides its slope-forming character, is the abundance of pale yellowish-brown (10YR 6/2) to yellowish-gray (5Y 8/1) beds. The upper unit is composed dominantly of medium- to thick-bedded, medium light-gray (N6) limestone with abundant chert knots and lenses.

Abundant crinoid plates and less abundant echinoid spines were found in the lower, slope-forming unit. The only diagnostic fossil found, however, was a deformed *Dicryoclostus*(?) brachiopod valve of probable Permian age.

The contact of Kaibab Limestone with the underlying Coconino Sandstone is conformable and depositional in nature. Clasts of quartzite from the Coconino Sandstone are contained within Kaibab Limestone strata at this contact.

Moenkopi Formation(?)

Approximately 300 m of quartzite, phyllite, and minor conglomerate of the Triassic Moenkopi Formation(?) crop out along the southern margin of the sedimentary block (fig. 3). This formation crops out as a series of small hills to the south of the main mass of Kaibab Limestone. The Moenkopi Formation(?) is a very heterogeneous unit. Only the major rock types found in the map area are described below.



Figure 6. Cascade fold in Supai Formation. View is to the southwest, towards Little Harquahala Mountains.

The lower third of this formation is made up dominantly of pyrite-bearing quartzites. Color on fresh surfaces ranges from light gray (N7) to light brown (5YR 6/4) to grayish green (10GY 5/2). Black desert varnish covers most exposed surfaces. Euhedral pyrite cubes, to 2 mm in size, are dispersed throughout these quartzites.

The dominant rock type overlying the quartzite is finely foliated phyllite which comprises approximately two-thirds of the formation. This phyllite is typically medium gray (N6) and has growths of green chlorite plates on foliation surfaces. A 3 m conglomerate bed was found in the lower portion of the phyllite unit. In this conglomerate, sub-rounded pebbles up to 4 cm in length and smaller rock fragments lie within a chloritized, fine-grained matrix. The larger pebbles observed were exclusively quartzite. Smaller pebbles and rock fragments are also dominantly quartzitic with minor amounts of feldspar. Color on most exposed surfaces of this conglomeratic bed is dark greenish gray (5G 4/1). A 2 m thick bed of dolomite was found immediately below the conglomerate. This dolomite is grayish orange (10YR 7/4) on weathered surfaces and moderate red (5R 5/4) on fresh surfaces. Thin chert layers define a fine lamination in this bed.

Nowhere in the map area was a depositional contact observed between the Moenkopi Formation(?) and the underlying Kaibab Limestone. The only contact between these two formations is the low-angle fault located just west of the Hidden Treasure Fault (fig. 3). However, the Moenkopi Formation(?) is assumed to overlie the Kaibab Limestone along a contact located somewhere beneath the alluvium which separates outcrops of the two units.

CORRELATION OF SEDIMENTARY UNITS

The Harquahala Mountains lie within an area which has been termed the "Arizona Sag" by Eardley (1949). During the Paleozoic, this area was a slowly sinking shelf which lay between the Defiance Positive Area and the so-called Ensenada Land (McKee, 1951). (See fig. 9.) This sag connected the Cordilleran and Sonoran Geosynclines during Paleozoic time (McKee, 1951). Thus, the stratigraphic record in this area may possess rocks with both southeastern Arizona and Colorado Plateau affinities. Because of the paucity of fossils within the rocks of the Harquahala Mountains, correlation of stratigraphic units is based primarily on lithologic similarity and stratigraphic sequence. It is the opinion of the writer that the stratigraphy of the Harquahala Mountains can be reconciled using present Arizona stratigraphic nomenclature.



Figure 7. Large-scale crossbedding in Coconino Sandstone.

Kaibab Limestone, Coconino Sandstone, Supai Formation

The three-fold conformable sequence of pale red quartzites overlain by vitreous, crossbedded quartzites, in turn overlain by varicolored, cherty limestone appears remarkably similar to upper Paleozoic strata known to the north in the Colorado Plateau region. Specifically, the descriptions of the Supai Formation, Coconino Sandstone, and Kaibab Limestone closely match those of this three-fold sequence, whereas a similar correlation to the strata of southeastern Arizona cannot be made.

Noble (1922) and more recently McKee (1975) have described the Pennsylvanian-Permian Supai Formation as consisting of flat to crossbedded, reddish sandstones with minor limestone and shale interbeds. Conformably overlying the Supai Formation at the Grand Canyon is the Hermit Shale (Noble, 1922). However, to the south, in the vicinity of Jerome-Oak Creek Canyon, Arizona (fig. 10), the Hermit Shale is not present (Anderson and Creasey, 1958) and its absence there is explained by a facies change south of the Grand Canyon (H.W. Peirce, personal comm.). There is no correlative to the Hermit Shale in the Harquahala Mountains and it is suggested that its absence is probably explained by such a facies change. The Permian Coconino Sandstone (Darton, 1910; McKee, 1934) on the Colorado Plateau is a very conspicuous formation consisting of vitreous white to gray sandstone which possesses large-scale crossbedding. Conformably overlying the Coconino Sandstone is the Permian Kaibab Limestone (Darton, 1910) consisting of gray- to buff-colored, cherty limestone and sandstone. The lower Kaibab Limestone has been designated the Toroweap Limestone by McKee (1938). However, the distinction of this subdivision as a mappable formation is not always made. (For example see Moore, 1972.)

The closest match of the three-fold sequence to southeastern Arizona stratigraphic nomenclature is the Permian sequence Concha Limestone and Scherrer Formation (fig. 10). The Concha Limestone is described as a massive-bedded, cherty, gray limestone (Bryant, 1968). The Scherrer Formation underlies the Concha Limestone and consists of two massive, white to brown sandstone units separated by a dolomitic limestone unit (Bryant, 1968). A basal red siltstone is locally present.

The Concha Limestone and Scherrer Formation may be correlative to the varicolored, cherty limestone and vitreous quartzite units of the three-fold, conformable sequence. However, in detail, the lithologic match would be rather tenuous. Also, the lower reddish quartzites are not represented in the southeastern Arizona rock record as the Scherrer Formation overlies thousands of feet of Cambrian to Permian limestone with only minor sandstone strata present (fig. 10).

In summary, it is felt that the thick sequence of quartzites overlain by varicolored, cherty limestone in the Harquahala

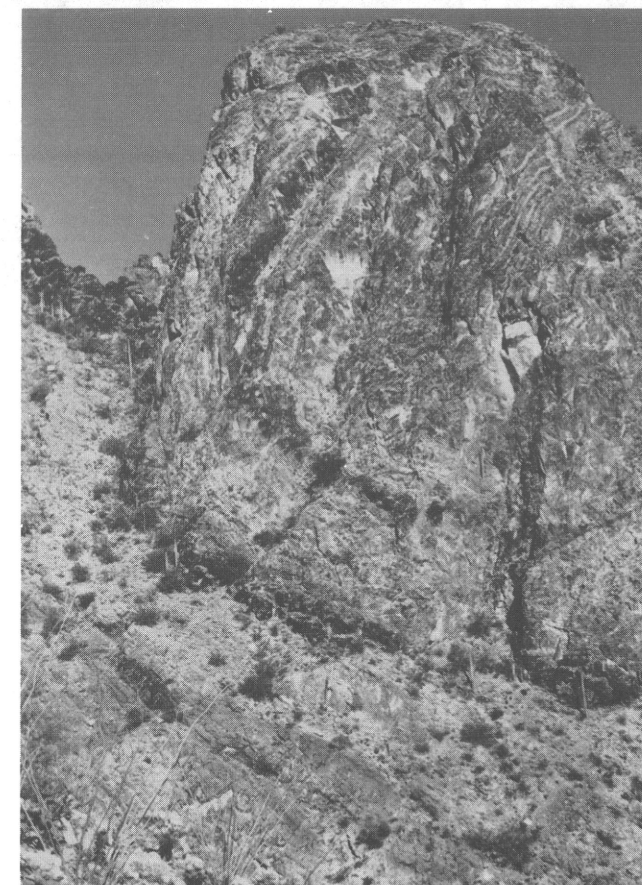


Figure 8. Macroscopic fold in Kaibab Limestone. View is to the northeast. Sense of overturning of fold is to the southeast. Saguaro cacti at base of hill give scale.

Mountains is lithologically and stratigraphically equivalent to the Colorado Plateau sequence of Supai Formation, Coconino Sandstone, and Kaibab Limestone. Miller (1966, 1970), working 50 km to the west in the Plomosa Mountains (fig. 10), recognized an identical upper Paleozoic sequence.

Redwall Limestone

With the above correlation established, it is possible to evaluate the remaining stratigraphic units in the Harquahala Mountains.

Immediately underlying the quartzites of the Supai Formation in the map area is a pink to red dolomite unit. As was previously mentioned, the contact between the quartzite and dolomite is a fault which cuts out a white, cherty marble unit to varying degrees. This bedding-plane fault was not observed during reconnaissance in the Little Harquahala Mountains (fig. 1). The contact there appears to be conformable and lithologic relationships within this "complete" section suggest that separation along the above mentioned fault is not large. The dolomite unit is therefore considered to be stratigraphically the youngest unit beneath the Supai Formation with the white marble unit representing merely a thin, upper part of the same formation.

LEASQUIT, INC.

Project: Little Harguabala North

Drill Hole: LHN-84-1

Grid Location: _____

Collar Elevation: _____

Drill Log Forms

Drillers: Drilling Services Co

Logged By: C. Lake

Start: 9/11/84

Finish: 9/13/84

Survey:	Depth	Bearing	D
	Collar		90°

____ core from _____ to _____
 ____ core from _____ to _____
 ____ core from _____ to _____

P.1

Scale	Structure Alteration	Rock Type	Rock Descriptions	Description of Mineralization, Alteration, Structures	Recovery	Sample Interval	Assays	
							Au	Ag
			Alluvium					
10								
20			Lms. Pink, gray to black, banded & mottled. Calcite veinlets	Recrystallized to vfg marble				
30					100	10901	<.005	ND
40			<u>Water table</u>		100	10902	<.005	ND
50					100	10903	<.005	ND
60					100	10904	<.005	ND
70					100	10905	<.005	ND
80			Lms. Reddish brown w/ 1-2% black material	Recrystallized. Cut by irregular thin calcite fractures	100	10906	<.005	T
					100	10907	<.005	ND
					100	10908	<.005	ND
					100	10909	<.005	ND
					100	10910	<.005	ND
					100	10911	<.005	ND

ALL VALUES IN OZS/t

P.2

Rock Descriptions

Description of Mineralization, Alteration, Structures

Assays ALL VALUES IN OZS

Sec	Stru	Alter	Rock	Rock Descriptions	Description of Mineralization, Alteration, Structures	Recovery	Sample	Inte	Assays	
									Av	Ag
				Reddish brown lms. 1-2% black lms. some material has shaly texture. Red material more becoming siltstone	Recrystallized. Traces lt gray sericite? Granitic appearing material may be calc. g.	100	10912	<.005	T	
90				Increasing amount of black lms. 60-40 Red calcareous siltstn to black foliated lms	recrystallized w/ very dense calcite filled hairline fractures. Numerous fractures filled w/ black calcite or siderite	100	10913	<.005	T	
				siltstone. Red-brown. Calcareous abundant black inclusions		100	10914	<.005	ND	
100						100	10915	.005	T	←
						100	10916	<.005	T	
110						100	10917	<.005	T	
						100	10918	<.005	ND	
120				Black MnO ₂ mixed red brown calcareous siltstone.	Botryoidal pyrolusite. Fills fractures. Comprises up to 80% of sample.	100	10919	<.005	T	
						100	10920	<.005	T	
130				Lt gray v. or gr quartz ^{Minor} calcareous material	Sericite. Lt gray gray appears to occur along bedding planes.	100	10921	<.005	T	
						100	10922	<.005	T	
140				v. or gr becomes more lt gray in color	U.F.-br. specular hematite imparts gray color	100	10923	<.005	.6	←
						100	10924	<.005	ND	
150						100	10925	<.005	T	
						100	10926	<.005	T	
160						100	10927	<.005	ND	
					160 Traces of hematite along fracture surfaces. Non calcareous. Some secondary gtz veining	100	10928	<.005	ND	
170				v. or gr becomes pink w/ increasing hematite. Sericite + chlorite fill fractures & coat surfaces. Larger pieces show intense brecciation		100	10929	.008	T	←
						100	10930	.022	ND	←
180						100	10931	<.005	ND	

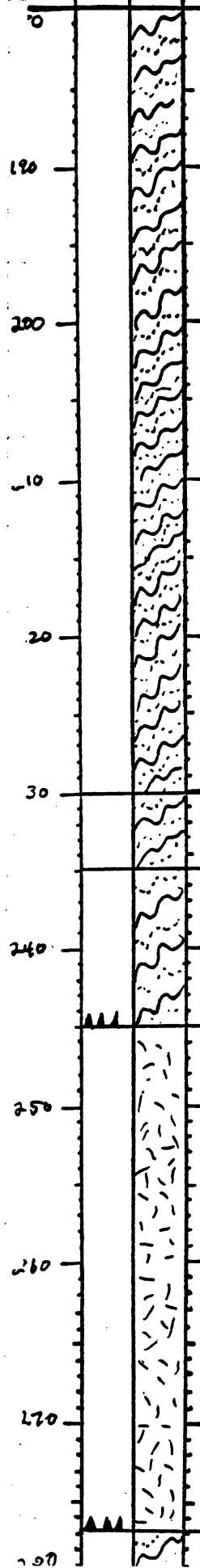
LHN- 84-1

P.3

Rock Descriptions

Description of Mineralization, Alteration, Structures

Recovery	Sample Interval	ASSAYS	
		Au	Ag
100	10932	<.005	ND
100	10933	<.005	ND
100	10934	<.005	ND
100	10935	<.005	ND
100	10936	<.005	T
100	10937	<.005	ND
100	10938	<.005	ND
100	10939	<.005	ND
100	10940	<.005	ND
100	10941	<.005	ND
100	10942	<.005	ND
100	10943	<.005	ND
100	10944	<.005	ND
100	10945	<.005	ND
100	10946	<.005	ND
100	10947	<.005	ND
100	10948	<.005	ND
100	10949	<.005	ND
100	10950	<.005	ND
100	10951	<.005	ND



Red-green quartzite. Siderite + gang. chloritic + sericitic shears. Some black hematite veins.

Color becomes redish gray

Quartzite becomes dk gray w/ red hematitic ~~mineral~~ disseminations

Quartzite, Lt gray, traces of hematite on frac surfaces

unit becomes red-gray

Great dk gray + dk green gray chlorite granite, Intensely btd. frags of sericitized mylonitic? material

gray to green intensely btd quartzite, fine grained. chlorite - chloritic + sericitic

200 Abundant red hematite in fracs + disseminations.

Some MnOx on fracture surfaces

Some FeOx + MnOx on frac surfaces chlorite + sericite in fractures

240 Increasing amount of hematite on grain surfaces

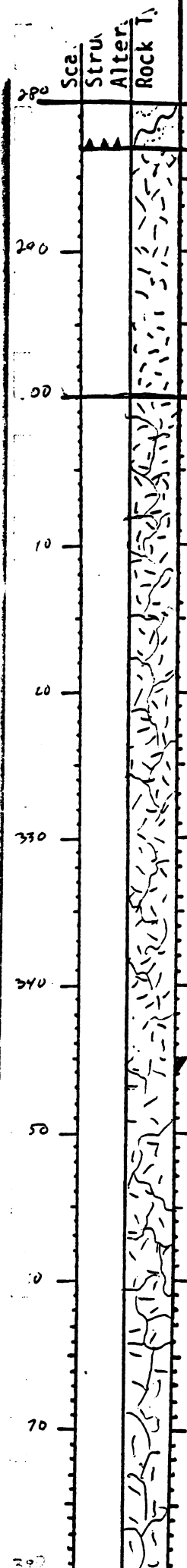
FeOx in fracs.

Siderite along dense basal frac

L7111 0 1-1
P.4

Description of Mineralization, Alteration, Structures

Assay ALL VALUES IN OZS./T



Rock Descriptions

CONTACT Approx. Granite. Gray to greenish gray. Intensely fractured & brecciated. Sinterized green gray flsrs. Some flsrs milky. Matrix altered to black sooty material

Pink & light green gray brecciated granite cloudy flsrs. Clots of green scapolite appear to form in matrix of bra

Change to tricoquelit

unit becomes more clayey. Clay is light tan to pink & sandy. Unit apparently intensely brecciated

Siderite along hairline fracs & in bra matrix

abundant hematite, brown siderite. mafics altered to sooty texture

Accounting some pink & tan clay in sample - apparently bra matrix

Recovery	Sample	Int'l	Au	Ag
✓	10952	<	.005	T
✓	10953	<	.005	T
✓	10954	<	.005	T
✓	10955	<	.005	T
✓	10956	<	.005	T
✓	10957	<	.005	T
✓	10958	<	.005	T
✓	10959	<	.005	T
✓	10960	<	.005	T
✓	10961	<	.005	T
✓	10962	<	.005	T
✓	10963	<	.005	T
✓	10964	<	.005	0.5
✓	10965	<	.005	ND
✓	10966	<	.005	T
✓	10967	<	.005	ND
✓	10968	<	.005	ND
✓	10969	<	.005	T
✓	10970	<	.005	T
✓	10971	<	.005	ND

Scale	Struc	Alter	Rock T ₁	LHM-84-1 P.5 Rock Descriptions	Description of Mineralization, Alteration, Structures	Recovery	Sample Interval	Assays		ALL VALUES IN OZS./	
								AU	Ag		
22						✓	10972	<.005	T		
						✓	10973	<.005	T		
390						✓	10974	<.005	ND		
						✓	10975	<.005	ND		
400						✓	10976	<.005	ND		
				Slightly increasing amount of chlorite + tan clay		✓	10977	<.005	ND		
410						✓	10978	<.005	ND		
				Granite. Tan. 50% Tan clay. Cloudy Flrs. No Biotics. Intensely argillized.	Hematite along frak + surfaces. Contains traces of siderite	✓	10979	<.005	ND		
420						✓	10980	<.005	T		
						✓	10981	<.005	T		
430				white bull gtz vein		✓	10982	<.005	T		
						✓	10983	<.005	ND		
440						✓	10984	<.005	T		
						✓	10985	<.005	T		
450				Bright red brown hematitic granite. Abundant red-brown + tan clay in matrix	Contains siderite in frak + on grain surfaces.	✓	10986	<.005	T		
						✓	10987	<.005	ND		
460				Tan granite. Cloudy Flrs. Chlorite. Lt graygy sericitic matrix. Abundant Tan clay. In matrix	Siderite abundant	✓	10988	<.005	T		
						✓	10989	<.005	ND		
470						✓	10990	<.005	ND		
						✓	10991	<.005	ND		

LHMV - 07-1

P.6

Rock Descriptions

Description of Mineralization, Alteration, Structures

Recovery Sample Interval

Assays

ALL VALUES IN OZS./T

Sec	Stru.	Alter.	Rock T ₁	Rock Descriptions	Description of Mineralization, Alteration, Structures	Recovery Sample Interval	Au	Ag			
480											
490											
500											
510											
520											
530											
540											
550											
560											
570											

Some component becoming more white.

Minor traces of MnO₂. None Fe₂O₃ or SiO₂.

Tan granite, some clay, clay portion tan & orange, some clay, clay fibers. Homoflex some fine chlorite

Siderite, hematite, Limonite

Material becoming more tan to brown white clay

Brecciated granite, slightly darker color than above, some tan clay, abundant chlorite fragments, some as carbonate.

Minor pyroxene, some Mn

Brown, some tan or reddish brown hematite 50%. Abundant hematite coats grains in matrix, red color to sample

Siderite in clay in veinlets.

Brecciated tan granite & clay, some clay as above

Siderite hematite

Granite approx 70% white clay, intensely altered.

Minor carbonate, traces of red hematite & brown siderite.

Unit contains abundant red hematite on surfaces imparting red color, some white clay

Minor siderite in veinlets in clay

View Looking West

LHN-84-1

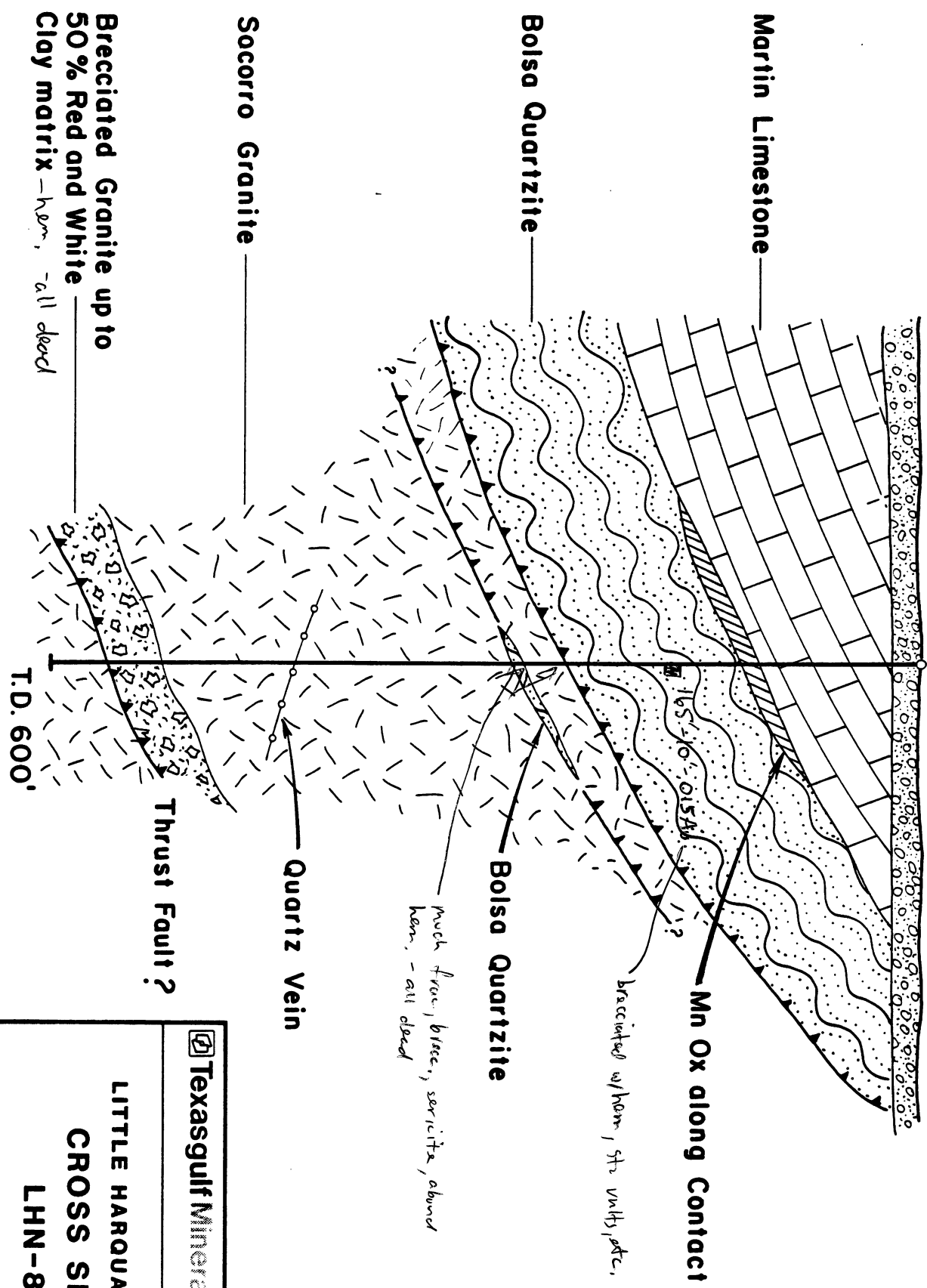


FIG. 4

 Texasgulf Minerals and Metals, Inc.	
LITTLE HAROUAHALA NORTH CROSS SECTION LHN-84-1	
Scale: 1 Inch equals 100 feet	Date by: C. LANE
Drafted by: Asplund	Oct. 21, 1985

Texasquit, Inc.

Project: Little Harguahala North

Drill Hole: LHN-84-2

Grid Location: _____

Collar Elevation: _____

Drill Log Forms

Drillers: Drilling Services Inc

Logged By: C. Lane

Start: 9/13/84

Finish: _____

Survey: _____

Depth	Bearing	Dip
Collar		90'

____ core from _____ to _____
 ____ core from _____ to _____
 ____ core from _____ to _____

P1

Scale	Structure Alteration	Rock Type	Rock Descriptions	Description of Mineralization, Alteration, Structures	Recovery Sample Interval	Assays				
			Alluvium			Assays Begin at 340 ALL VALUES IN OZS./TON				
0										
20										
40										
60										
80										
100										
120										
140										
160										
180										
200										
220										
240										
260										
280										
300										
320										
340										
360										
380										
400										
420										
440										
460										
480										
500										
520										
540										
560										
580										
600										
620										
640										
660										
680										
700										
720										
740										
760										
780										
800										
820										
840										
860										
880										
900										
920										
940										
960										
980										
1000										

11020 Pistachio green granite. Some ^{usual} green gray material included

11021 some carbonate. Traces of black biotite or very dark chlorite

11016

11017

11018

11019

11020

11021

11022

11023

11024

11025

11026

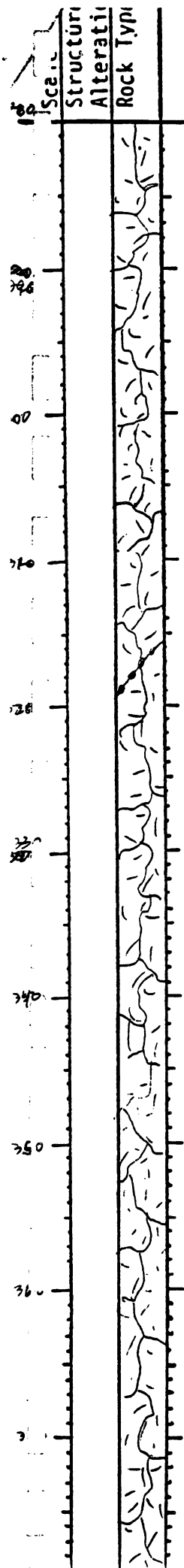
Scale	Structure	Alteration	Rock Type	LHN-84-2 P.2 Rock Descriptions	Description of Mineralization, Alteration, Structures	Recovery	Sample	Interval	Assays				
90				Quartz re. above		/	11027						
90					Traces of red hematite as discrete grains & disseminated specks	/	11028						
100				water table		/	11029						
100						/	11030						
100						/	11031						
110						/	11032						
110					Unit becomes olive drab color. Hematitic material occurs as clots that are epigenetic	/	11033						
120						/	11034						
120						/	11035						
130						-	11036						
130						/	11037						
140						/	11038						
140						/	11039						
150				Pinkish brown amphibolite. Fresh bituminous cloudy fibers	Pistachio green pyrite coating into sample.	/	11040						
150						/	11041						
160						/	11042						
160						/	11043						
170						✓	11044						
170							11045						
170							11046						

UNALTERED

Tv

Scale	Structure	Alteration	Rock Type	Rock Descriptions	Description of Mineralization, Alteration, Structures	Recovery	Sample Interval	Assays						
								Au	Ag					
100				Pink Andesite as above		✓	11047							
110						✓	11048							
120				Light gray volcanic tuff. SS. white to light gray clay matrix. 20% particles of pink to red brown unaltered dacite	Chlorite + biotite	✓	11049							
130						✓	11050							
140						✓	11051							
150						✓	11052							
160	Argillite				Unit becomes more tuffaceous at base 1/3.	✓	11053							
170				Reddish brown andesite tuff. Clayey groundmass. Cloudy f.l.s. Biotite subhedral to slightly ragged. Some chlorite in biotite		✓	11054							
180						✓	11055							
190						✓	11056							
200						✓	11057							
210						✓	11058							
220						✓	11059	<.005	T					
230						✓	11060	<.005	T					
240							11061	<.005	T					
250				congl? mostly clay			11062	<.005	T					
260							11063	<.005	T					
270				Granite. Tan to reddish brown. f.l.s. cloudy. Abundant chlorite in grains + in matrix. Traces of MnO ₂ on grain surfaces. Intensely brecciated	Siderite fills hairline fracs + occupies matrix		11064	<.005	0.6					
280							11065	<.005	T					
290							11066	<.005	T					

ALL VALUES IN OZS/T



LIV 07-2
P.4

Rock Descriptions

overall color change to Lt green

white bull getz vein

Description of Mineralization, Alteration, Structures

small white bull getz veins from 285-295

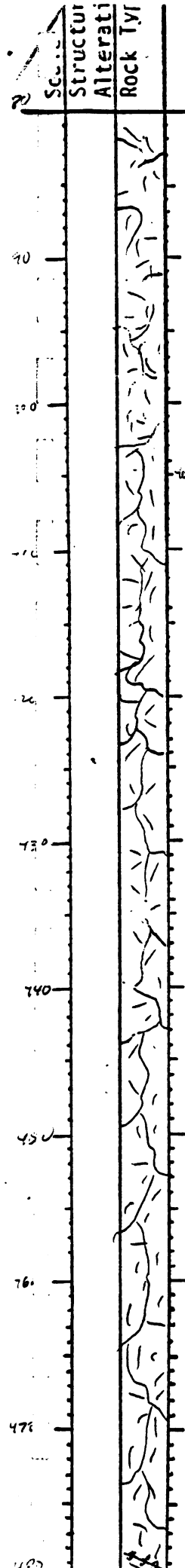
305-310 Feldspars sericitized (light green)

310 - abundant siderite imparts brown color to granite. Decrease in amt of Lt green sericite.

340. Siderite comprises 2.50% of sample

Some secondary getz veining - trace

Recovery	Sample	Ints ^{avg}	Assays		ALL VALUES IN OZS./TON		
			Av	Ag			
	11067	<	.005	ND			
	11068	<	.005	0.5			
	11069	<	.005	0.5			
	11070	<	.005	0.8			
	11071	<	.005	0.7			
	11072	<	.005	ND			
	11073	<	.005	T			
	11074		.011	T			
	11075		.052	T			
	11076	<	.005	ND			
	11077	<	.005	T			
	11078	<	.005	T			
	11079	<	.005	T			
	11080	<	.005	ND			
	11081	<	.005	ND			
	11082	<	.005	T			
	11083	<	.005	ND			
	11084	<	.005	T			
	11085	<	.005	ND			
	11086	<	.005	ND			



P.5
Rock Descriptions

Color gradually changes to tan or brown
increase in limonite - brown siderite

overall color more rusty brown

Description of Mineralization, Alteration, Structures

some white bulgite. Limonite or goethite
pores after pyrite. Siderite in veinlets
traces of black Mn. Oxide grains in sulfates

40% - 45% becomes light gray overall color.
Minor limonite + siderite

increase in siderite content

white bull + 2 veins

Recovery	Sample	Inte:	Assays			
			ALL VALUES IN OZS./TON			
			Au	Ag		
	11087	<	.005	ND		
	11088	<	.007	ND		
	11089	<	.005	T		
	11090	<	.005	ND		
	11091	<	.099	T		
	11092	<	.075	ND		
	11093	<	.005	T		
	11094	<	.005	T		
	11095	<	.005	T		
	11096	<	.005	T		
	11097	<	.005	T		
	11098	<	.005	ND		
	11099	<	.005	ND		
	11100	<	.005	ND		
	11101	<	.005	ND		
	11102	<	.005	ND		
	11103	<	.005	ND		
	11104	<	.005	ND		
	11105	<	.005	ND		
	11106	<	.005	ND		

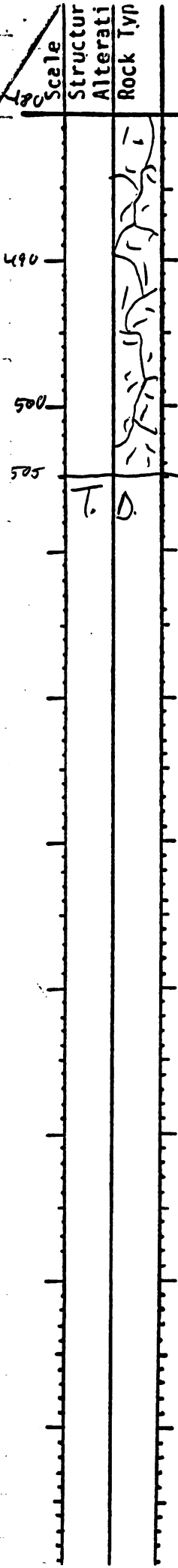
LTV 11/87 ✓

P.6

Rock Descriptions

Description of Mineralization, Alteration, Structures

Recovery Sample Interval Assays ALL VALUES IN OZS./T



Brecciated granite as above

Recovery Sample Interval	Assays		ALL VALUES IN OZS./T	
	Au	Ag		
11107	0.07	ND		
11108	<.005	ND		
11109	<.005	ND		
11110	.007	ND		
11111	<.005	ND		

T.D.

View Looking West

LHN-84-2

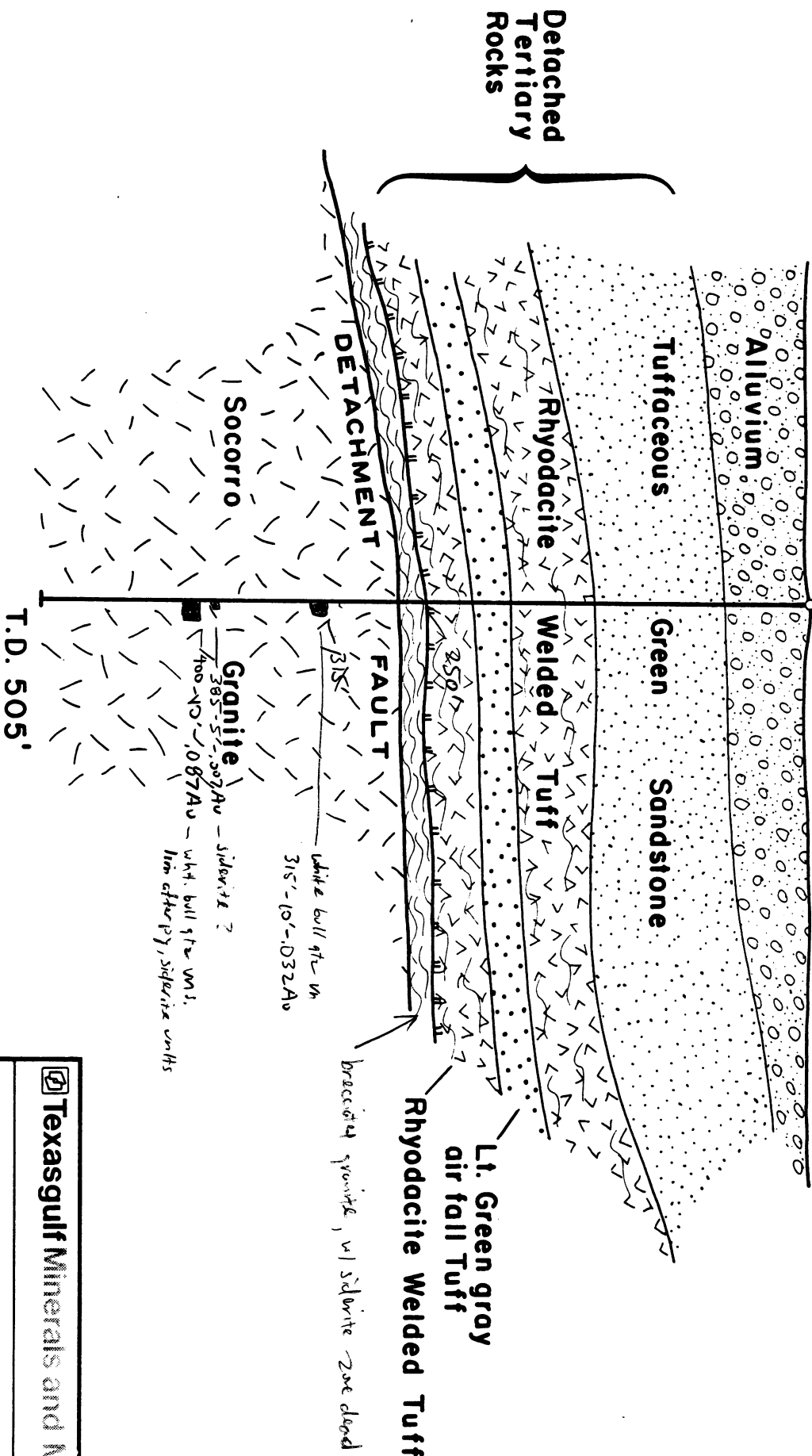


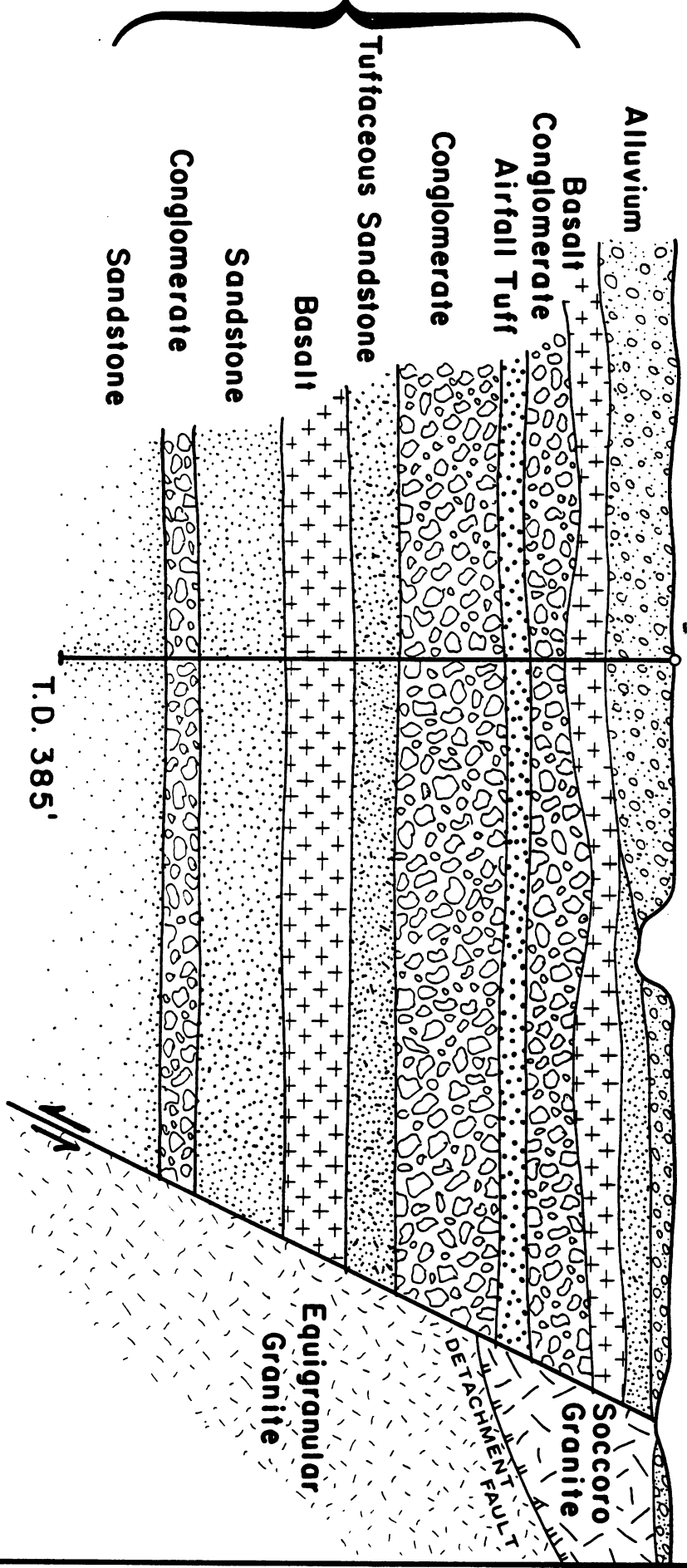
FIG.5

Texasgulf Minerals and Metals, Inc.	
LITTLE HAROUAHALA NORTH	
CROSS SECTION LHN-84-2	
Scale: 1 inch equals 100 feet	Date by: C. LANE
Drafted by: Asplund	Oct. 21, 1985

View Looking West

LHN-84-3

DETACHED TERTIARY ROCKS



Texasgulf Minerals and Metals, Inc.

LITTLE HARQUAHALA NORTH

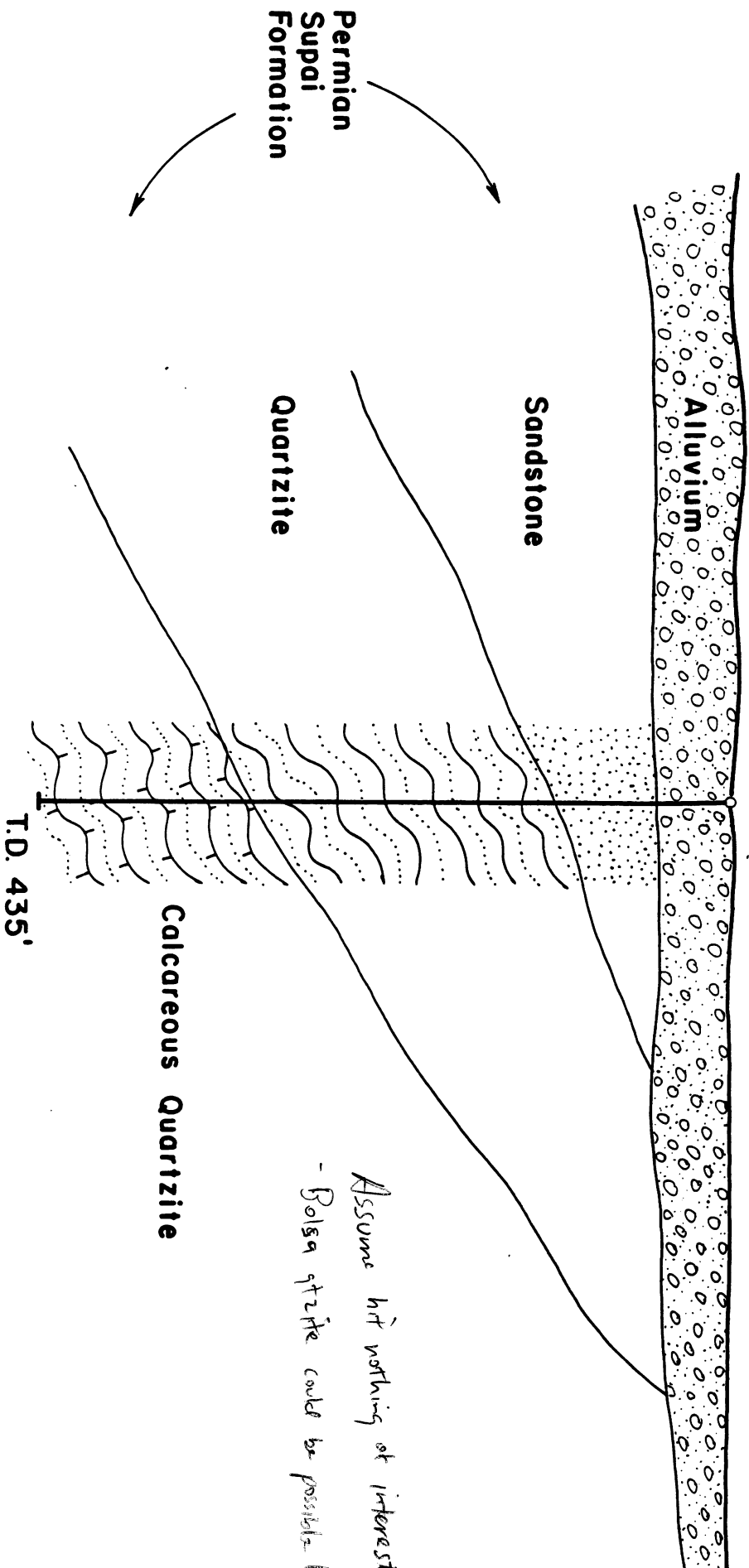
CROSS SECTION LHN-84-3

FIG. 6

Scale: 1 inch equals 100 feet
 Drafted By: Asplund | Oct. 21, 1985
 Date By: C. LANE

View Looking West

LHN-84-4



*Assume hit nothing of interest
- Bolsa quartzite could be possible host.*

Texasgulf Minerals and Metals, Inc.
LITTLE HARQUAHALA NORTH
CROSS SECTION LHN-84-4

FIG. 7

Scale: 1 inch equals 100 feet	Date by: C. LANE
Drafted by: Asplund	Oct. 21, 1985

Texasgulf, Inc.

Project: Unit 1 Little Hogue/Abbe

Drill Hole: LHN 851

Grid Location: _____

Collar Elevation: _____

Drill Log Forms

Drillers: Drilling Services Co.

Logged By: C. Lantz

Start: 3/12/85

Finish: _____

Survey: _____

____ core from _____ to _____
 ____ core from _____ to _____
 ____ core from _____ to _____

Depth	Bearing	Dip
Collar		

Scale	Structure Alteration	Rock Type	Rock Descriptions	Description of Mineralization, Alteration, Structures	Recovery	Sample Interval	Assays					
							Ar	Ag				
0			Alluvium									
30			Brecciated Sericitic granite, white & tan gangue & red brown rhyolite (may be calc. altered)	Sericitized chloritic matrix + feldsp. weak CO ₂ . Abundant chlorite								
45			45 - Red brown rhyolitic material no longer present.									
50												
55												
60												
65												
70												
75												
80												
85												
90												
95												
100												
105												
110												
115												
120												
125												
130												
135												
140												
145												
150												
155												
160												
165												
170												
175												
180												
185												
190												
195												
200												
205												
210												
215												
220												
225												
230												
235												
240												
245												
250												
255												
260												
265												
270												
275												
280												
285												
290												
295												
300												
305												
310												
315												
320												
325												
330												
335												
340												
345												
350												
355												
360												
365												
370												
375												
380												
385												
390												
395												
400												
405												
410												
415												
420												
425												
430												
435												
440												
445												
450												
455												
460												
465												
470												
475												
480												
485												
490												
495												
500												

ALL VALUES IN PPM

Sericite, Chlorite, Carbonate

30 - clay gangue / silicified gr

Sec	Struct	Alteration	Rock Typ	LHN- 85-1	Description of Mineralization, Alteration, Structures	Recovery Sample Interval	ALL VALUES IN P			
							Au	Ag		
				85 - large silicified - tan and	80 - Large grey silicified granite Sericite. Sericite + Qtz veins in blue grey chalcidony 85 - Increase in chlorite content Fw corroded hemipyr pseudos K + CO ₂	11831	.09	.3		
70						11832	.01	4.2		
						11833	2.01	4.2		
80						11834	2.01	4.2		
						11835	2.01	4.2		
110						11836	2.01	4.2		
						11837	2.01	4.2		
120					120-130 decrease in chlorite Olivine color in gangue	11838	2.01	4.2		
						11839	2.01	4.2		
130				130 granite - tan and brown K + CO ₂ + sericite	130 - Increase in hem op fracture coatings. Increase in chlorite. Pure hemipyr pseudos	11840	.04	4.2		
						11841	2.01	4.2		
140						11842	2.01	4.2		
						11843	.01	4.2		
150						11844	2.01	4.2		
						11845	.09	4.2		
160						11846	.01	4.2		
						11847	2.01	4.2		
170						11848	0.11	.4		
						11849	2.01	4.2		
180						11850	1.0	4.2		

OK .7

Scale	Structure	Alteration	Rock Type	LHN 85 1	Description of Mineralization, Alteration, Structures	Recovery	Sample Interval	ALL VALUES IN PPM					
								Au	Ag				
							11851	.04	4.2				
							11852	4.01	4.2				
							11853	.08	4.2				
							11854	.06	4.2				
							11855	.04	4.2				
							11856	.01	4.2				
							11857	.01	4.2				
							11858	4.01	4.2				
					200-236 Local zone 30-300m of vein ag in 2-2 portion of granite. Ken hem chlorite in matrix. Some scoria.		11859	.01	4.2				
					200-236 25m long vein zone in granite. Some scoria. S. 11859-11860		11860	4.01	4.2				
							11861	4.01	4.2				
							11862	4.01	4.2				
							11863	4.01	4.2				
							11864	4.01	4.2				
							11865	4.01	4.2				
							11866	.08	4.2				
							11867	4.01	4.2				
							11868	.03	4.2				
					200-236 outcrop changes to massive granite hematite + FeO ₂ . High Fe content in granite		11869	4.01	4.2				
							11870	.01	4.2				

LHS-85-1

ALL VALUES IN PPM

Sec.	Struct.	Alteration	Rock Type	Rock Descriptions	Description of Mineralization, Alteration, Structures	Recovery	Sample Interval	ALL VALUES IN PPM	
								Au	Ag
				Granite on road	350 ft				
							11871	4.01	4.2
							11872	.04	4.2
							11873	.03	.2
							11874	.05	4.2
300							11875	.02	4.2
				370 color change to green to dark green	30-320 color change due to increase in chlorite & green hematite		11876	.02	4.2
							11877	.01	4.2
320				320 color change to yellow brown & green.	Unit contains abundant hematite & brown Fe ₂ O ₃ . Sulfide green chlorite. Some pyrite & arsenic.		11878	.03	4.2
							11879	.01	4.2
							11880	4.01	4.2
330					330 Increase in hematite on Bullhead red hematite & arsenic. Hematite in section. Hematite produces weak silicification. Sulfide in matrix & replacing fides.		11881	.02	4.2
							11882	4.01	.2
							11883	.02	4.2
							11884	.01	4.2
							11885	.03	4.2
							11886	.05	4.2
340							11887	.07	4.2
							11888	4.01	4.2
370							11889	.02	4.2
380							11890	4.01	4.2

Weak Silicification with Sulfide

ALL VALUES IN P

Sca. Struct. Alteration Rock Type	LHN 85.1 Rock Descriptions	Description of Mineralization, Alteration, Structures	Recovery Sample Interval	Au Ag						
	<p>390 - Trace Fresh Pyrite</p>		1181	.01	<.2					
			1182	6.01	<.2					
			1183	6.01	<.2					
			1184	.01	<.2					
			1185	.02	<.2					
			1186	6.01	<.2					
			1187	.01	<.2					
			1188	.01	<.2					
			1189	6.01	<.2					
			1190	6.01	<.2					
			1191	6.01	<.2					
			1192	6.01	<.2					
		<p>440 - slight color change from 460 : swarthy -> more crystalline due to leaching</p>		1193	6.01	<.2				
				1194	.04	<.2				
				1195	.03	<.2				
				1196	.07	<.2				
				1197	.02	<.2				
				1198	.01	<.2				
				1199	6.01	<.2				
				1200	.03	<.2				

460 color change to light green

460 465 abundant light green
silica

LHN-85

Description of Mineralization, Alteration, Structures

ALL VALUES IN PP

Scale
Structural
Alteration
Rock Type

Rock Descriptions

Recovery	Sample Interval	ALL VALUES IN PP	
		μ	Ag
	11911	.02	<.2
	11912	.03	<.2
	11913	.05	<.2
	11914	.02	<.2
	11915	4.01	<.2
	11916	4.01	<.2
	11917	.01	<.2
	11918	4.01	<.2
	11919	4.01	<.2
	11920	4.01	<.2
	11921	4.01	<.2
	11922	4.01	<.2
	11923	4.01	<.2
	11924	.01	<.2
	11925	4.01	<.2
	11926	4.01	<.2
	11927	4.01	<.2
	11928	4.01	<.2
	11929	4.01	<.2
	11930	4.01	<.2

Granite as above

as above

505- Dark green granite

505- color change due to Abundant iron oxide, Trace hematite. Weave of fine iron. Numerous hematite pseudomorphs. Abundant iron FeCO₃

525- Dark green granite

525- Dark green granite. Abundant iron oxide. Trace hematite. Weave of fine iron. Numerous hematite pseudomorphs.

Transition zone

Transition zone. Abundant iron oxide. Trace hematite. Weave of fine iron. Numerous hematite pseudomorphs.

Sericite - Chlorite - Hematite - Carbonate



View Looking North

LHN-85-1

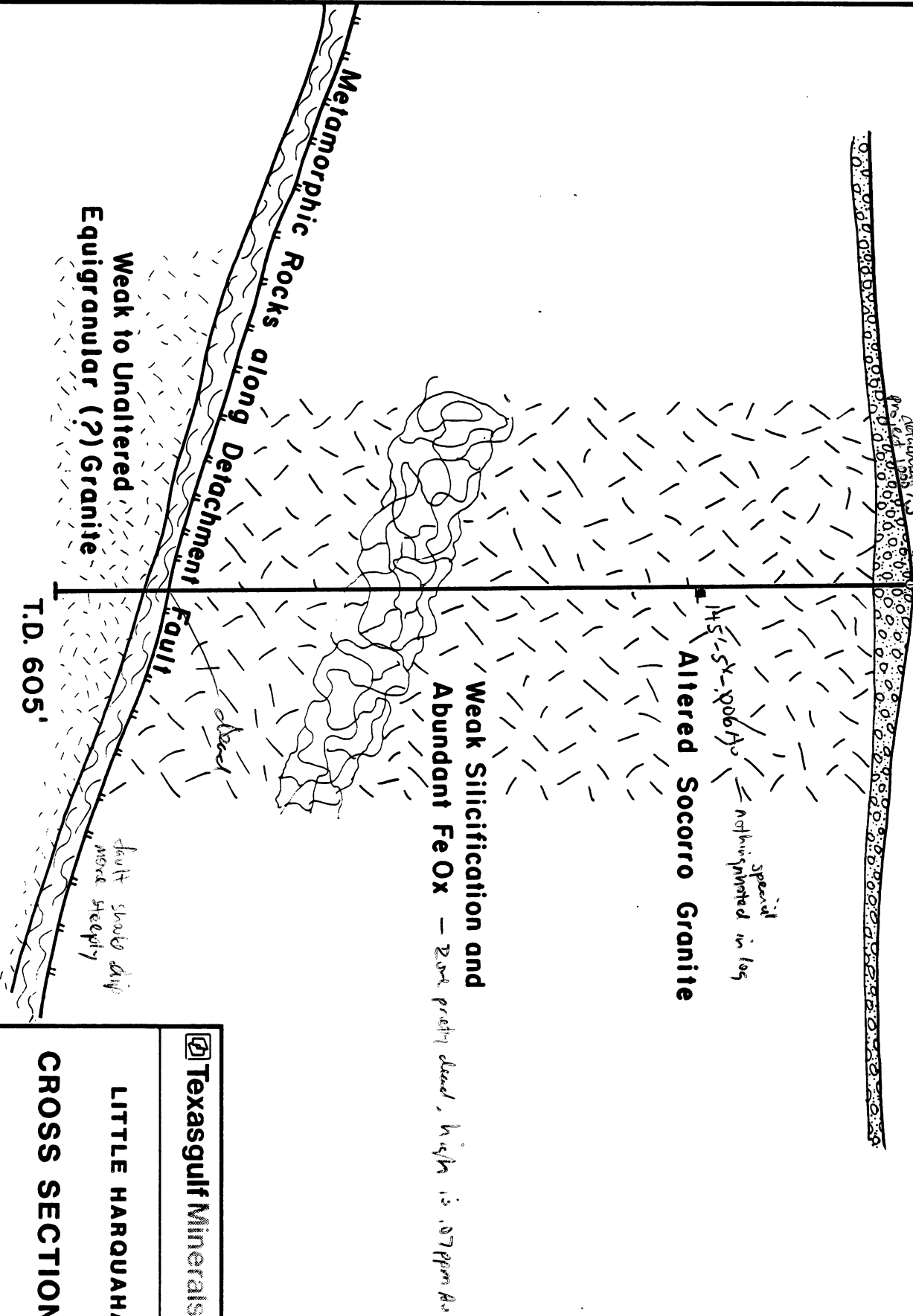


FIG. 8

Texasgulf Minerals and Metals, Inc.	
LITTLE HARQUAHALA NORTH	
CROSS SECTION LHN-85-1	
Scale: 1 inch equals 100 feet Drafted By: Asplund Oct. 21, 1985	Date By: C. LANE

Texasgulf, Inc.

Drill Log Forms

Project: Little Harguakola North

Drillers: Drilling Services Co.

Drill Hole: LHM-85-2

Logged By: C. Long

Grid Location: _____

Start: 3/20/85

Collar Elevation: _____

Finish: _____

_____ core from _____ to _____
 _____ core from _____ to _____
 _____ core from _____ to _____

Survey:	Depth	Bearing	Dip
	Collar		90°

cal	Structure Alteration Rock Type	Rock Descriptions	Description of Mineralization, Alteration, Structures	Recovery Sample Interval	ALL VALUES IN PPM				
					Av	A _g			
0									
10									
20									
30									
40									
50									
55		Granite - Lt grey with white & pinkish brown	Sericite (grey) matrix. Matrix cemented by yellow brown CO ₂	5600	6.0	2.3			
60				5610	6.0	2.2			
65			55-60 Brown, red brown, yellow brown color due to abundant Fe in matrix	5611	6.0	2.2			
70			60-65 limonite hematitic clay fault gouge	5612	6.0	1.5			
75		65 - overall color change to pinkish brown + grey	Few small hematite nodules, hematite in thin fracs, Lt grey sericitic matrix is blue grey quartz.	5613	6.0	2.2			
80				5614	6.0	2.2			
85				5615	6.0	2.2			